

Correlation-guided Query-Dependency Calibration in Video Representation Learning for Temporal Grounding

WonJun Moon, Sangeek Hyun, SuBeen Lee, Jae-Pil Heo*
 Sungkyunkwan University

{wjun0830, hsi1032, leesb7426, jaepilheo}@g.skku.edu

Abstract

Recent endeavors in video temporal grounding enforce strong cross-modal interactions through attention mechanisms to overcome the modality gap between video and text query. However, previous works treat all video clips equally regardless of their semantic relevance with the text query in attention modules. In this paper, our goal is to provide clues for query-associated video clips within the cross-modal encoding process. With our Correlation-Guided DEtection TRansformer (CG-DETR), we explore the appropriate clip-wise degree of cross-modal interactions and how to exploit such degrees for prediction. First, we design an adaptive cross-attention layer with dummy tokens. Dummy tokens conditioned by text query take a portion of the attention weights, preventing irrelevant video clips from being represented by the text query. Yet, not all word tokens equally inherit the text query’s correlation to video clips. Thus, we further guide the cross-attention map by inferring the fine-grained correlation between video clips and words. We enable this by learning a joint embedding space for high-level concepts, i.e., moment and sentence level, and inferring the clip-word correlation. Lastly, we use a moment-adaptive saliency detector to exploit each video clip’s degrees of text engagement. We validate the superiority of CG-DETR with the state-of-the-art results on various benchmarks for both moment retrieval and highlight detection. Codes are available at github.com/wjun0830/CGDETR.

1. Introduction

Video temporal grounding is to detect temporal moments that align with user-specified language requests. Aside from the moment localization, recent works also explore how well each video clip corresponds with the text query. To address these tasks, it is crucial to align the representation space across modalities. In this regard, the use of transformers [64] has become a common approach that facilitates easy integration of multimodal representations. While

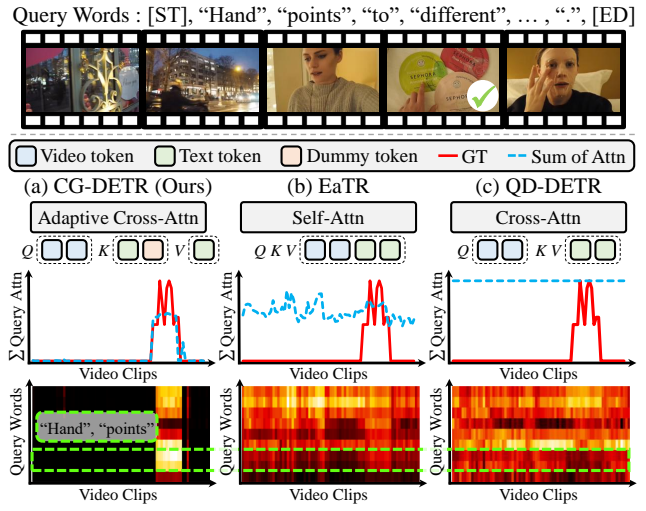


Figure 1. Comparison of degrees of text-to-video correlation in attention layers. In the middle row, we compare the clip-wise correspondence score to the text query (sum of attention weights over all words) with its corresponding GT (saliency scores). While the use of (b) self-attention or (c) cross-attention fails to distinguish target clips based on the degree of cross-modal attention, our approach (a) exhibits a high activation level for the text query to attend only the query-relevant clips since the dummies occupy a portion of the attention degree on irrelevant clips. We also investigate the fine-grained correlation between clips and words. Despite the absence of supervision, our method learns to attend more to salient words.

some studies [32, 43] use transformer encoders to establish a shared embedding space, others also leverage detection transformers for making predictions [27, 71]. Recently, QD-DETR [46] highlighted previous works’ insufficient text reflection in predictions and suggested explicitly forcing text engagement with cross-attention. Yet, in moment retrieval scenarios where users seek specific video segments, we argue that uncalibrated text involvement in each video clip also has a large stake in insufficient text engagement. We suggest that the adaptive textual conditioning on each clip enables the model to attend to desired moments based on the degree of text condition, thereby maintaining the high text involvement across all video clips may not necessarily be the optimal solution. In Fig. 1, we display the clip-wise degree of cross-modal attention. Although only a few clips

* Corresponding author

are relevant to the given query, previous works using (b) self-attention and (c) cross-attention exhibit similar degrees of cross-modal interaction on every clip both in terms of the entire query and each word. For the importance of the adaptive degree in attention, we examine the positive relationship between the alignment of clip-wise query attention degrees with the corresponding ground truth (GT) saliency scores and their impact on performance in Appendix A.1.

Building upon the observation that the exploration for optimal cross-modal interaction among visual and texture representations remains a yet-to-be-explored challenge in temporal grounding, our Correlation-Guided DEtection TRansformer (CG-DETR) focuses on discovering the appropriate degree of interaction and utilizing such degrees in predictions. To this end, we first propose an Adaptive Cross-Attention layer (ACA) that modifies the operation of the cross-attention layer; by adding dummy tokens to the *key* in the multi-head attention, we adjust the intensity of text query’s clip-wise engagement based on the relevance between video clips and a text query. Subsequently, we delve into the relationship between clips and each word in a text query. It is evident that not all words bear close relevance to a video clip, even if they are part of a highly relevant text query. Still, studying a fine-grained correlation is demanding since word-level supervision requires huge resources. Thus, we approximate the clip-word relevance by calculating similarity in a modality-aligned space at a more coarse video and sentence level. The similarity map is then, distilled to adjust the magnitude of the attention map in the cross-attention layer. Lastly, whereas previous saliency detectors rely on learnable parameters, we propose a moment-adaptive saliency detector that leverages the magnitude of the cross-modal interaction. A saliency token designed with two principles, *i.e.*, preserving original context and representing diverse characteristics of desired moments, is aggregated with textual information. This allows us to incorporate scaled interaction degrees into prediction.

To sum up, our contributions are (i) We propose adaptive cross-attention with dummy tokens to enable the manipulation in the degree of video-text interaction with respect to their correlation, (ii) To further calibrate the interaction degree, we discover and distill the clip-word correlation from the aligned space at video-sentence level, (iii) We introduce a moment-adaptive saliency detector to exploit the calibrated degree of cross-modal interaction, and (iv) Extensive experiments demonstrate the effectiveness of CG-DETR.

2. Related Work

2.1. Video Temporal Grounding

Video temporal grounding, a task to link the text query to corresponding video segments, can be further divided into moment retrieval and highlight detection which localizes the desired moments and scores the clip-wise correspondence

to the query. Moment retrieval has been introduced with the goal of retrieving user-desired moments [1, 10, 15, 33, 34, 59, 78]. Conventional approaches fall into either proposal-based or proposal-free methods. Proposal-based methods employ predefined proposals, *e.g.*, sliding windows [1, 16, 38, 77, 82] and temporal anchors [8, 35, 77, 79, 85], or learn to generate proposals [37, 56, 67, 69, 84] to prepare moment candidates. With the candidates, they treat the task as the matching problem between candidates and the text query. On the other hand, proposal-free methods learn to encode multimodal knowledge and predict the temporal spans with the regression head. Highlight detection aims to score the importance of every clip with respect to either visual or textual information. It has been studied extensively with varying sources, *e.g.*, visual only [4, 54, 68, 70] and visual-audio [3, 19, 21, 68], and different granularity levels on the given labels; there exist supervised [18, 63, 70], weakly supervised [6, 49, 68], and unsupervised methods [4, 25, 45, 53] for highlight detection.

Recently, since the advent of QVHighlights [27], these problems are now being considered together. Since then, newly proposed approaches can be divided into DETR- or regression-based. Employing either streams, diverse kinds of practices were conducted; UMT [43] exploited additional audio modality, QD-DETR [46] and EaTR [23] developed the DETR architecture, and [32, 72] remarked the importance of pretraining. Also, the study for the query dependency is being spotlighted [5, 20, 39, 46, 86]. Our motivation resembles these works, especially QD-DETR [46]. However, whereas they only focus on enforcing text engagement in every video clip, we aim to discover an appropriate degree and calibrate the query dependency in cross-modal interaction.

2.2. Vision-text Alignment

Driven by the recognition that learning the joint embedding spaces for visual and textual modalities yields effective representations, there has been a surge of interest in vision-text alignment [24, 28–31, 50, 75, 76]. Subsequently, outcomes of the studies have been introduced in multimodal downstream tasks, *e.g.*, CLIP has gained prominence for video grounding. However, even large pretrained models do not invariably possess a perfect shared embedding space. Hence, efforts have been directed toward refining cross-modal interactions in downstream tasks to address such limitations. In the context of video grounding, dual contrastive learning [48] and multimodal reasoning [88] have been proposed to improve text-video alignment. Similarly, QD-DETR [46] employed negative-pair learning to learn general relationships and fostered active cross-modal interaction. Our work strives for a more precise understanding of relations. Subsequent to forming an aligned space between the video and sentence, we infer fine-grained clip-word similarity within the space, enabling the manipulation of the behavior of cross-modal interaction for enhanced video temporal grounding.

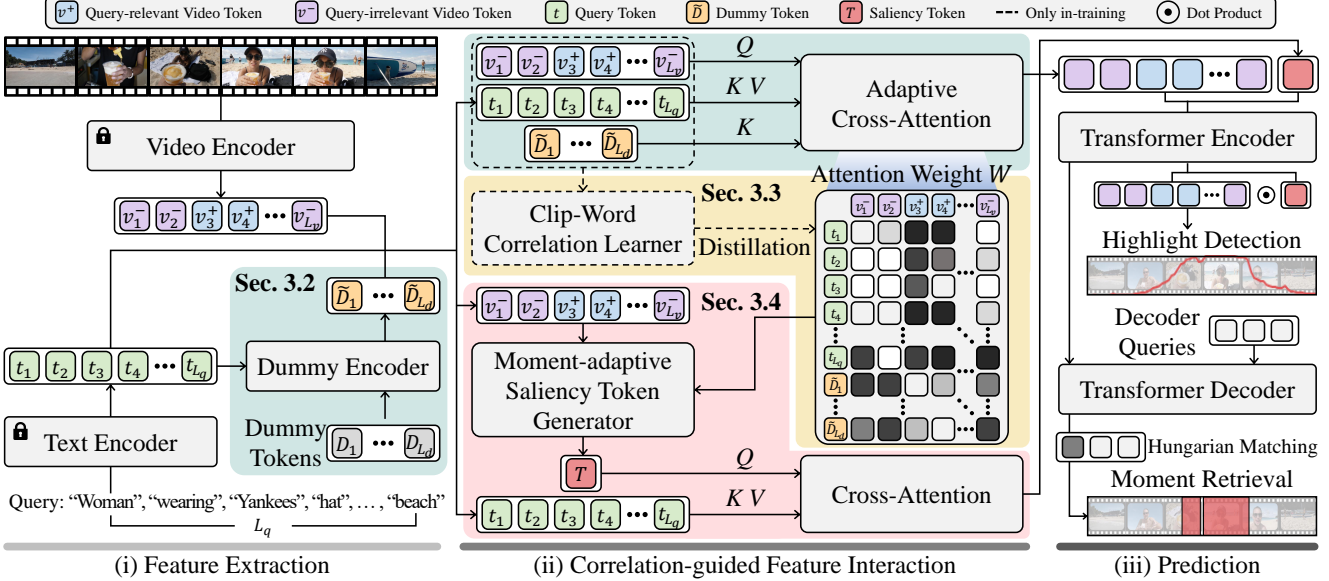


Figure 2. An overview of CG-DETR. From left to right, the model consists of three phases: (i) feature extraction, (ii) correlation-guided feature interaction, and (iii) predictions for grounding tasks. (i) Along with video and text feature extraction, dummy tokens are conditioned by the query to represent the query-excluding meaning. (ii) Correlation-guided feature interaction is performed with adaptive cross-attention. In addition to calibration of text query engagement as a whole, we also guide the word-wise engagement with the clip-word correlation learner. At the bottom, we utilize the video context and a calibrated attention map to generate a saliency token. A saliency token is processed through the same cross-attention layer to be similarly encoded with video tokens to prevent a modality gap. Details for correlation learner and saliency token are in Fig. 4, 5. (iii) Finally, tokens are processed through the encoder and decoder to make predictions.

3. Method

3.1. Overview

Given a video $V = [v_1, \dots, v_{L_v}]$ of L_v clips and a text query $Q = [q_1, \dots, q_{L_q}]$ of L_q tokens, our objective is to predict clip-wise saliency scores $\{s_1, s_2, \dots, s_{L_v}\}$ and to localize the target moments in the form of (m_c, m_σ) where m_c and m_σ denote the center temporal coordinate and span of the moment. The overview of our model is illustrated in Fig. 2.

The aim of CG-DETR is to leverage the interrelation between modalities to improve the feature interaction operation. To achieve that, in Sec. 3.2, we propose to employ the dummy tokens D ; these serve to distinguish the degree of cross-modal attention for each video clip and are conditioned by query tokens to encapsulate representations that exclude query contexts. In Sec. 3.3, we provide fine-grained correlation guidance to the adaptive cross-attention layers by aligning the modalities at the video-sentence level where supervision is available and inferring at a more granular clip-word level. Lastly, in Sec. 3.4, we introduce a saliency token that incorporates both video context and moment-adaptive knowledge derived from clip-wise query correspondence in the learned attention map of cross-attention layers. Then, a saliency token processed via cross-attention exclusively with text tokens is concatenated with clip-wise tokens to be forwarded for the prediction.

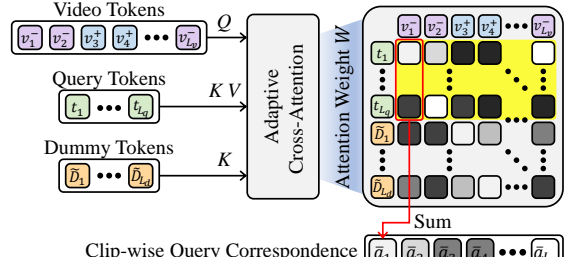


Figure 3. Illustration of deriving clip-wise query correspondence \bar{a} .

3.2. Adaptive Cross-Attention: Reflecting the Video-Text Correlation

Adaptive cross-attention stems from the insight that not all contents in a video always correspond to the semantics of a text query. Meanwhile, cross-attention is one of the most popular methods to incorporate the features of different modalities, especially for retrieval tasks [46, 60]. Yet, as the softmax applied in the cross-attention forces the text query to be equally aggregated across all video clips, the cross-attention is inadequate to learn the degree of video-text correspondence. A naïve solution is to change the softmax activation to sigmoid. However, we point out the vulnerability of sigmoid in ranking the text-relevance scores of clips since it eliminates the dependency among other clips.

Instead, we introduce dummy tokens that are concatenated to the text tokens and possess a portion of attention weights in cross-attention layers. Assuming that we have L_d

learnable dummy tokens $D = [D_1, \dots, D_{L_d}]$, these dummy tokens are conditioned by the text query Q through attention layers to contain the query-excluding context. We denote the encoded dummy tokens as \tilde{D} . Then, in the cross-attention layer where *query* $Q = [p_Q(v_1), \dots, p_Q(v_{L_v})]$ and *value* $V = [p_V(t_1), \dots, p_V(t_{L_q})]$ are prepared by projecting the video clips and text queries, dummy tokens take part in *key* $K = [p_K(t_1), \dots, p_K(t_{L_q}), p_K(\tilde{D}_1), \dots, p_K(\tilde{D}_{L_d})]$, concatenated with text tokens before *key* projection. $p_Q(\cdot)$, $p_K(\cdot)$, and $p_V(\cdot)$ are projection layers for *query*, *key*, and *value*. Formally, the operation of adaptive cross-attention with dummy tokens for i -th video clip, $\text{ACA}(v_i)$, is expressed as:

$$\text{ACA}(v_i) = \sum_{j=1}^{L_q} W_{i,j} \odot V_j; W_{i,j} = \frac{\exp\left(\frac{Q_i \odot K_j}{\sqrt{h}}\right)}{\sum_{k=1}^{L_q+L_d} \exp\left(\frac{Q_i \odot K_k}{\sqrt{h}}\right)}, \quad (1)$$

where h denotes the projected hidden dimension and \odot stands for the dot product. To guide the dummy tokens to take desired portions of attention weights that are inversely proportional to the saliency scores, we define a query correspondence score for i -th clip, $\bar{a}_i = \sum_{j=1}^{L_q} W_{i,j}$, as shown in Fig. 3 and train \bar{a}_i by applying the objectives for highlight detection. Details for the objective are in Sec. 3.5 and Appendix A.4. In addition, we employ binary cross-entropy to discretize between moment and non-moments within every instance and enforce orthogonality among encoded dummy tokens to prevent them from playing the same role:

$$\mathcal{L}_{\text{bce}} = \frac{1}{L_v} \sum_{i=1}^{L_v} (a_i \odot \log \bar{a}_i + (1 - a_i) \odot \log (1 - \bar{a}_i)), \quad (2)$$

$$\mathcal{L}_{\text{ortho}} = \frac{1}{L_d(L_d - 1)} \sum_{m=1}^{L_d} \sum_{n=1}^{L_d} \mathbb{1}_{m \neq n} |\tilde{D}_m \odot \tilde{D}_n|, \quad (3)$$

where a_i is 1 if the saliency GT is non-zero, otherwise set to 0. By allowing such flexible cross-attention, the model learns better separation of relevant and irrelevant video segments.

3.3. Clip-Word Correlation Learner: Align, Discover, and Distill the Fine-grained Correlation

By employing ACA, the model considers the clip-wise relevance with text query. Delving into the clip-word relation, it is evident that not all words are equally associated with visual clues. With this motivation, we further aim to discover the proper attention weights for cross-attention that represent the correlation between video clips and semantic words.

However, determining the proper clip-word correlation is challenging in the absence of supervision. Hence, we take a two-step approach; 1) learning the vision-text-aligned embedding space at the video-query level where supervision is given, 2) inferring the vision-text correlation at a more fine-grained level, *i.e.*, clip-word level, and distill the correlation to the attention map in the cross-attention layers.

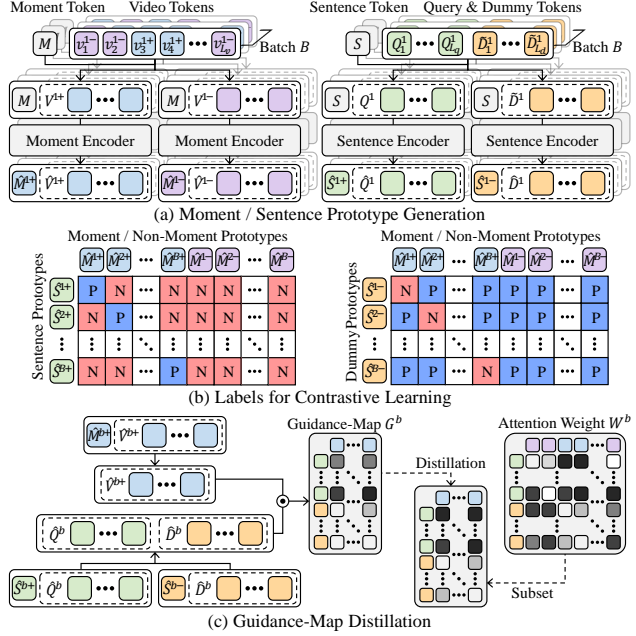


Figure 4. Clip-word correlation learner. We discover and reflect the relevance between clips and text words into cross-attention. (a) We establish visual moment, non-moment, query, and dummy representative tokens (\hat{M}^{b+} , \hat{M}^{b-} , \hat{S}^{b+} , and \hat{S}^{b-}) using learnable moment and sentence tokens. (b) To learn the aligned space, we implement contrastive learning. Whereas the text query prototype \hat{S}^b learns to be aligned with the paired visual moment token \hat{M}^b , dummy prototype \hat{S}^b learn to exclude the moment-specific knowledge. (c) Within the aligned space, the correlation in clip-word level is employed as the guidance for the attention map in the cross-attention.

To align the embedding space of both modalities at a video-sentence level, we generate moment and non-moment prototypes for both modality domains with domain-specific prototype tokens, *i.e.*, moment and sentence tokens, and apply contrastive learning between them [11, 31, 41, 50]. Let $V^{b+} = [v_i^b | i \in \{1, 2, \dots, L_v\}, a_i = 1]$ and $V^{b-} = [v_i^b | i \in \{1, 2, \dots, L_v\}, a_i \neq 1]$ be the video clips in the specified target moment (query-relevant) and otherwise (query-irrelevant) in b -th video instance of batch size B , respectively. As mentioned in Sec. 3.2, a indicates the GT for query correspondence score \bar{a} . In Fig. 4 (a), we illustrate prototype generation. By processing learnable moment token M with each of these visual inputs through the self-attention block (SA), we derive moment prototype \hat{M}^{b+} and non-moment prototypes \hat{M}^{b-} for b -th video instance in the visual domain each with the projected video representations \hat{V}^{b+} and \hat{V}^{b-} :

$$\hat{M}^{b+}, \hat{V}^{b+} = \text{SA}([M; V^{b+}], [M; V^{b+}], [M; V^{b+}]), \quad (4)$$

$$\hat{M}^{b-}, \hat{V}^{b-} = \text{SA}([M; V^{b-}], [M; V^{b-}], [M; V^{b-}]), \quad (5)$$

where $[;]$ and $\hat{\cdot}$ denote concatenation and projected output via SA, respectively. Symmetrical to processing the moment token M in the video domain, we leverage the learnable sentence token S with each of the b -th text query Q^b and dummy

tokens D^b to yield moment and non-moment prototypes in the semantic domain:

$$\hat{S}^{b+}, \hat{Q}^b = \text{SA}([S; Q^b], [S; Q^b], [S; Q^b]), \quad (6)$$

$$\hat{S}^{b-}, \hat{D}^b = \text{SA}([S; \tilde{D}^b], [S; \tilde{D}^b], [S; \tilde{D}^b]). \quad (7)$$

Consequently, with \mathcal{B} as the index set in the batch, we formulate the contrastive learning objective for b -th instance using the batch-wise labels in Fig. 4 (b):

$$\mathcal{L}_{\text{align}}^+ = -\log \frac{\exp(\hat{S}^{b+} \odot \hat{M}^{b+}/\tau)}{\sum_{a \in \mathcal{B}} \sum_{* \in \{+, -\}} \exp(\hat{S}^{b+} \odot \hat{M}^{a*}/\tau)}, \quad (8)$$

$$\mathcal{L}_{\text{align}}^- = -\log \left(1 - \frac{\exp(\hat{S}^{b-} \odot \hat{M}^{b-}/\tau)}{\sum_{a \in \mathcal{B}} \sum_{* \in \{+, -\}} \exp(\hat{S}^{b-} \odot \hat{M}^{a*}/\tau)} \right), \quad (9)$$

$$\mathcal{L}_{\text{align}} = \mathcal{L}_{\text{align}}^+ + \mathcal{L}_{\text{align}}^-. \quad (10)$$

To illustrate, $\mathcal{L}_{\text{align}}^+$ is to enforce the proximity between the visual moment prototypes \hat{M}^{b+} and semantic moment prototypes \hat{S}^{b+} whereas $\mathcal{L}_{\text{align}}^-$ is to assign the moment-excluding visual representation in the dummy tokens. The design choice for assigning such a large semantic coverage in the dummy tokens is due to the obscurity of the opposite meaning in terms of high-dimensional moment and sentence space. For instance, the sentence consists of words and there exist opposite terms for every word which makes it hard to define the opposite definition of the high-dimensional sentence. Hence, we instead learn the dummy tokens to cover large semantics that excludes only the particular semantics.

Then, we infer the word-clip correlation from the aligned space to derive the guidance G (Fig. 4 (c)) for the attention map in the adaptive cross-attention layer:

$$G_{i,j} = \frac{\exp(\hat{v}_i^+ \odot [\hat{Q}; \hat{D}]_j)}{\sum_{k=1}^{L_q+L_d} \exp(\hat{v}_i^+ \odot [\hat{Q}; \hat{D}]_k)}, \quad (11)$$

where \hat{v}_i^+ is i -th video clip of \hat{V}^+ . Note that we only derive the guidance for positive clips, *i.e.*, clips belonging to the GT moments, since the model has not learned the positive textual relationships for non-moment clips which can make it susceptible to inaccuracies. Finally, we provide clip-word level guidance to the attention map in the cross-attention layer. Given the weights in the attention map W defined in Eq. 1 and the guidance G defined in Eq. 11, distillation loss $\mathcal{L}_{\text{distill}}$ is expressed as:

$$\mathcal{L}_{\text{distill}} = \frac{1}{L_v} \sum_{i=1}^{L_v} \sum_{j=1}^{L_q+L_d} \mathbb{1}_{v_i \in V^+} W_{i,j} \log \frac{W_{i,j}}{G_{i,j}}. \quad (12)$$

Via establishing the shared semantic space at the video-sentence level and distilling the inferred clip-word correlation, we expect interpretable attention layers that also take the fine-grained semantics into account.

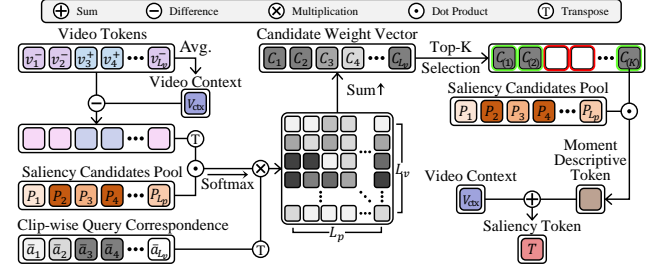


Figure 5. Saliency token generation. The saliency token is obtained by combining video-averaged context with a moment-descriptive token which is calculated by aggregating top-K moment-descriptive candidates. Specifically, we yield a moment-descriptive token by subtracting a context token from clip tokens and then, use their correlation to saliency candidates as the moment-descriptiveness scores after scaling with clip-wise query correspondence \bar{a} .

3.4. Moment-adaptive Saliency Detector

We have discussed ways to calibrate the magnitude of cross-modal interaction concerning the correlation between video and text modalities. Here, we introduce the novel design of the saliency detector that exploits the calibrated degree of cross-modal interaction in each clip representation.

Following [46], we employ a saliency token to estimate the saliency scores by computing the similarity. This implies that there should be no contextual discrepancy between a saliency token and video representations while a saliency token also should encapsulate the dynamic characteristics of moments, *e.g.*, actions, within each video for discrimination.

Accordingly, we combine a video context token and a moment-descriptive token to generate the saliency token as described in Fig. 5. We maintain the video context by utilizing the averaged video token so-called a context token V_{ctx} . Conversely, we identify a moment-descriptive token from learnable candidate pools P . To effectively incorporate distinct characteristics of varying moments using a set number of candidate tokens, we initiate by eliminating context from the video clips. Subsequently, weighted similarity matching is applied between L_v clip tokens and L_p candidates in the pool. The top-K candidates are then aggregated to construct a moment-descriptive token based on their similarity values. Formally, the process is expressed as:

$$C_j = \sum_{i=1}^{L_v} \bar{a}_i \cdot \frac{\exp((v_i - V_{\text{ctx}}) \odot P_j)}{\sum_{k=1}^{L_p} \exp((v_i - V_{\text{ctx}}) \odot P_k)}, \quad (13)$$

$$T = V_{\text{ctx}} + \sum_{j=1}^{L_p} \mathbb{1}_{C_j \in \{C_{(1)}, C_{(2)}, \dots, C_{(K)}\}} P_j \odot C_j, \quad (14)$$

where $C_{(k)}$ denotes the k -th biggest value in the candidate weight vector C and $\mathbb{1}$ is an indicator. Note that we use clip-wise query correspondence \bar{a} from the cross-attention map as a weight to assign greater significance to clips pertinent to the desired moment during weighted similarity matching.

Utilizing the generated saliency token, we carry out query aggregation via cross-attention that shares the parameter with

Split	test										val									
	MR					HD					MR					HD				
	R1		mAP			>= Very Good		R1		mAP			>= Very Good							
Method	@0.5	@0.7	@0.5	@0.75	Avg.	mAP	HIT@1	@0.5	@0.7	@0.5	@0.75	Avg.	mAP	HIT@1						
BeautyThumb [62]	-	-	-	-	-	14.36	20.88	-	-	-	-	-	-	-						
DVSE [42]	-	-	-	-	-	18.75	21.79	-	-	-	-	-	-	-						
MCN [1]	11.41	2.72	24.94	8.22	10.67	-	-	-	-	-	-	-	-	-						
CAL [12]	25.49	11.54	23.40	7.65	9.89	-	-	-	-	-	-	-	-	-						
XML [26]	41.83	30.35	44.63	31.73	32.14	34.49	55.25	-	-	-	-	-	-	-						
XML+[26]	46.69	33.46	47.89	34.67	34.90	35.38	55.06	-	-	-	-	-	-	-						
Moment-DETR [27]	52.89	33.02	54.82	29.40	30.73	35.69	55.60	53.94	34.84	-	-	32.20	35.65	55.55						
UMT [43]	56.23	41.18	53.38	37.01	36.12	38.18	59.99	60.26	44.26	-	-	38.59	39.85	64.19						
QD-DETR [46]	62.40	44.98	62.52	39.88	39.86	38.94	62.40	62.68	46.66	62.23	41.82	41.22	39.13	63.03						
UniVGT [32]	58.86	40.86	57.6	35.59	35.47	38.20	60.96	59.74	-	-	-	36.13	38.83	61.81						
EaTR [23]	-	-	-	-	-	-	-	61.36	45.79	61.86	41.91	41.74	37.15	58.65						
CG-DETR (Ours)	65.43	48.38	64.51	42.77	42.86	40.33	66.21	67.35	52.06	65.57	45.73	44.93	40.79	66.71						

Table 1. Performance comparison on QVHighlights *test* and *val* splits with the features from Slowfast and CLIP. We calculate the average mAP score with IoU thresholds ranging from 0.5 to 0.95 in 0.05 intervals.

Method	TACoS						Charades-STA					
	R@0.3	R@0.5	R@0.7	mIoU	R@0.3	R@0.5	R@0.7	mIoU				
2D-TAN [83]	40.01	27.99	12.92	27.22	58.76	46.02	27.50	41.25				
VSLNet [80]	35.54	23.54	13.15	24.99	60.30	42.69	24.14	41.58				
Moment-DETR [27]	37.97	24.67	11.97	25.49	65.83	52.07	30.59	45.54				
QD-DETR [46]	-	-	-	-	-	57.31	32.55	-				
LLaViLo [44]	-	-	-	-	-	55.72	33.43	-				
UniVTG [32]	51.44	34.97	17.35	33.60	70.81	58.01	35.65	50.10				
CG-DETR (Ours)	52.23	39.61	22.23	36.48	70.43	58.44	36.34	50.13				

Table 2. Results on moment retrieval datasets, *i.e.*, TACoS and Charades-STA. Video features are extracted using Slowfast and CLIP.

ACA. However, unlike the process with video tokens, we omit dummy tokens from *key* and engage in cross-attention exclusively with pure text query tokens. In this fashion, we expect the saliency detector to be equipped with query awareness and leverage a finely calibrated degree of query involvement in each clip token for saliency score prediction.

3.5. Training Objectives

Our proposed CG-DETR operates with losses for moment retrieval and highlight detection. Briefly, we employ L1, gIoU [52], and cross-entropy objectives for moment retrieval and use margin ranking loss, rank contrastive loss, and entropy loss for highlight detection. Also, as discussed in Sec. 3.2, we use the same highlight detection objectives on \bar{a} , the clip-wise query correspondence which is derived by adding the attention weights of cross-attention layers. To abbreviate the moment retrieval, highlight detection, and attention weights \bar{a} learning objectives as \mathcal{L}_{mr} and \mathcal{L}_{hl} , and $\mathcal{L}_{\text{attn}}$, our overall objective can be formulated as:

$$\mathcal{L}_{\text{obj}} = \mathcal{L}_{\text{mr}} + \lambda_{\text{hl}} (\mathcal{L}_{\text{hl}} + \mathcal{L}_{\text{attn}} + \mathcal{L}_{\text{bce}}) + \lambda_{\text{ortho}} \mathcal{L}_{\text{ortho}} + \lambda_{\text{align}} \mathcal{L}_{\text{align}} + \lambda_{\text{distill}} \mathcal{L}_{\text{distill}} \quad (15)$$

For further details, we refer to the Appendix A.4.

Method	R@0.5	R@0.7
SAP [9]	27.42	13.36
SM-RL [66]	24.36	11.17
2D-TAN [83]	40.94	22.85
FVMR [14]	42.36	24.14
APGN [36]	44.23	25.64
SSRN [87]	46.72	27.98
UMT† [43]	48.31	29.25
QD-DETR [46]	52.77	31.13
CG-DETR (Ours)	55.22	34.19

Table 3. Performances on Charades-STA with VGG backbone. † indicates the usage of additional audio modality.

4. Evaluation

To validate the generality of our proposed method, we conduct extensive experiments on video grounding datasets. We use three datasets for moment retrieval: QVHighlights [27], Charades-STA [15], and TACoS [51], and three for highlight detection: QVHighlights, TVSum [61], and Youtubehl [63]. For the type of feature extractor, we follow previous works [23, 27, 43, 46] for a fair comparison; we utilize Slowfast+CLIP [13, 50], I3D [7], and VGG [57] networks. We refer to Appendix A.3 for dataset details and evaluation metrics.

4.1. Comparison with the State-of-the-arts

For joint moment retrieval and highlight detection tasks on QVHighlights, we present comparisons to the state-of-the-art methods in Tab. 1. For a fair comparison between methods, numbers are reported with the test and validation splits, respectively (We leave cells blank if the results are not available). As observed, our proposed method outperforms previous state-of-the-art methods with notable margins, *e.g.*, 8% boosts in mAP for MR in both splits and 8% and 12% increase in R1@0.7. Our superior performance over baseline

Method	VT	VU	GA	MS	PK	PR	FM	BK	BT	DS	Avg.
sLSTM [81]	41.1	46.2	46.3	47.7	44.8	46.1	45.2	40.6	47.1	45.5	45.1
SG [45]	42.3	47.2	47.5	48.9	45.6	47.3	46.4	41.7	48.3	46.6	46.2
LIM-S [68]	55.9	42.9	61.2	54.0	60.3	47.5	43.2	66.3	69.1	62.6	56.3
Trailer [65]	61.3	54.6	65.7	60.8	59.1	70.1	58.2	64.7	65.6	68.1	62.8
SL-Module [70]	86.5	68.7	74.9	86.2	79.0	63.2	58.9	72.6	78.9	64.0	73.3
QD-DETR [46]	88.2	87.4	85.6	85.0	85.8	86.9	76.4	91.3	89.2	73.7	85.0
UniVTG [32]	83.9	85.1	89.0	80.1	84.6	81.4	70.9	91.7	73.5	69.3	81.0
MINI-Net [22]†	80.6	68.3	78.2	81.8	78.1	65.8	57.8	75.0	80.2	65.5	73.2
TCG [74]†	85.0	71.4	81.9	78.6	80.2	75.5	71.6	77.3	78.6	68.1	76.8
Joint-VA [2]†	83.7	57.3	78.5	86.1	80.1	69.2	70.0	73.0	97.4	67.5	76.3
UMT [43]†	87.5	81.5	88.2	78.8	81.4	87.0	76.0	86.9	84.4	79.6	83.1
CG-DETR (Ours)	86.9	88.8	94.8	87.7	86.7	89.6	74.8	93.3	89.2	75.9	86.8

Table 4. Highlight detection results on TVsum. † denotes the methods that utilize the audio modality.

methods in both tasks substantiates the importance of calibrating the degree of cross-modal interactions. Specifically, we believe that the roles of the transformer encoder and decoder become considerably streamlined as they process discretized features based on their relevance to the given query during the cross-modal interaction phase.

Tab. 2 and Tab. 3 present comparisons on moment retrieval datasets: TACoS and Charades-STA. Interestingly, we observe variations in the performance gap across different datasets compared to previous state-of-the-art methods. For instance, while our results are notably superior on QVHighlights, the margin is slightly reduced on TACoS and relatively small on Charades-STA. We attribute this phenomenon to different dataset characteristics. To illustrate, QVHighlights offers long context-rich queries, *e.g.*, *A woman in a blue coat sits and waves to the camera as a man in a lab coat takes a sample*. In contrast, other datasets feature relatively short and simple queries, *e.g.*, *a person sits in a chair*. In short, we observe that the performance improvements in our proposed method are more pronounced when diverse textual semantics are provided, *i.e.*, when more unique words with longer queries are given. For more detailed statistics and discussions, we refer to Appendix A.2.

Results for highlight detection benchmarks are reported in Tab. 4 and Tab. 5. Unlike the moment predictions made with decoder outputs, saliency scores for highlight detection are calculated with the encoder outputs. Not only does our work achieve state-of-the-art results compared to previous methods that utilize only the video modality but also exceeds methods that use additional audio modality.

4.2. Ablation Studies

In Tab. 6, we investigate the effectiveness of each component with a lighter version of CG-DETR. For baseline (a), we employ the DETR-based architecture [27, 40] with a negative pair learning strategy proposed by QD-DETR [46]. Rows (b), (c), and (d) clearly validate the benefits of each component; (b) discloses the importance of adjusting the degree of cross-modal interaction according to the relevance between

Method	Dog	Gym.	Par.	Ska.	Ski.	Sur.	Avg.
RRAE [73]	49.0	35.0	50.0	25.0	22.0	49.0	38.3
GIFs [18]	30.8	33.5	54.0	55.4	32.8	54.1	46.4
LSVM [63]	60.0	41.0	61.0	62.0	36.0	61.0	53.6
LIM-S [68]	57.9	41.7	67.0	57.8	48.6	65.1	56.4
SL-Module [70]	70.8	53.2	77.2	72.5	66.1	76.2	69.3
QD-DETR [46]	72.2	77.4	71.0	72.7	72.8	80.6	74.4
UniVTG [32]	71.8	76.5	73.9	73.3	73.2	82.2	75.2
MINI-Net [22]†	58.2	61.7	70.2	72.2	58.7	65.1	64.4
TCG [74]†	55.4	62.7	70.9	69.1	60.1	59.8	63.0
Joint-VA [2]†	64.5	71.9	80.8	62.0	73.2	78.3	71.8
UMT [43]†	65.9	75.2	81.6	71.8	72.3	82.7	74.9
CG-DETR (Ours)	76.3	76.1	70.0	76.0	75.1	81.9	75.9

Table 5. Highlight detection performances on Youtube-hl. † indicates the usage of audio modality.

video clip and text query, (c) further shows the fine-grained relevance consideration beyond sentence level brings additional benefits, and finally with the representations built on the discriminative degree of cross-modal interaction, we find that moment-adaptive saliency detector easily captures the highlight clips in (d). Also, we briefly give a short review of the impact of the increased capacity of the model in (e) following [23, 32]. For detailed examinations of model capacity w.r.t. the model size, number of dummy tokens, and number of prompt tokens, we refer to extensive ablation studies in Appendix A.5.

Further ablation is conducted in Tab. 7. To be specific, we test the effectiveness of the adaptiveness in the cross-attention layer and validate the design choice for the saliency detector. Comparing (I) and (II), we observe that granting the adaptivity to manipulate the degree of cross-modal interaction in the cross-attention layer leads to notable differences in numbers. For the saliency detector, we compare our design choice (V) with naïvely employing a learnable saliency token (III) [46] and using video-averaged context as the saliency detector. The dominance of (V) over (III) and (IV) clearly demonstrates the importance of focusing on both the context gap and the diverse nature of video moments.

	ACA	CCL	MSD	MR			HD			
				R1			mAP		>= Very Good	
				@0.5	@0.7	@0.5	@0.75	Avg.	mAP	HIT@1
(a)				58.9	39.0	58.4	34.4	35.4	39.0	62.4
(b)	✓			62.9	46.0	62.46	41.3	41.1	39.6	62.5
(c)	✓	✓		64.2	47.4	63.7	43.3	42.0	40.2	64.8
(d)	✓	✓	✓	65.3	50.3	64.2	43.5	42.8	40.3	65.9
(e)	✓	✓	✓	67.4	52.1	65.6	45.7	44.9	40.8	66.7

Table 6. Component analysis on QVHighlights *val* split. ACA, CCL, and MSD denote *adaptive cross-attention*, *clip-word correlation learner*, and *moment-adaptive saliency detector* introduced in Sec. 3.2, 3.3, and 3.4. With all components combined in (d), we search the hyperparameters, *i.e.*, number of dummy tokens and number of layers, to train our final model in (e).

	MR			HD						
	R1	mAP	>= Very Good	@0.5	@0.7	@0.5	@0.75	Avg.	mAP	HIT@1
Adaptiveness in cross-attention layer										
(I)	59.9	41.9	58.7	35.9	36.0	39.1	63.2			
(II)	62.9	46.0	62.5	41.3	41.1	39.6	62.5			
Saliency detector										
(III)	65.5	50.3	64.7	44.8	43.8	39.8	64.8			
(IV)	66.0	49.8	65.1	44.3	43.7	39.9	64.9			
(V)	67.4	52.1	65.6	45.7	44.9	40.8	66.7			

Table 7. Ablation studies on adaptive cross attention and saliency detector. Studies are conducted on QVHighlights *val* split.

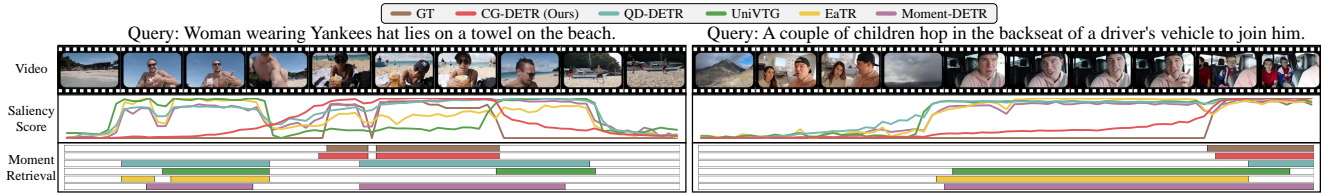


Figure 6. Visualization of prediction comparisons on QVHighlights.

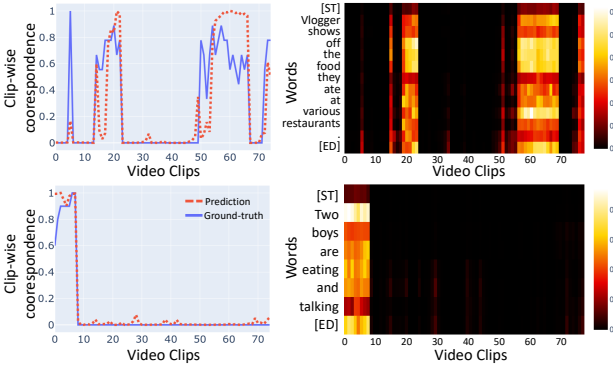


Figure 7. Examination of learned correlation between video clips and text query in CG-DETR. Each row comes from the same example. (Left) Comparison between the degrees of multimodal interaction and GT saliency scores. (Right) Learned correspondence between each word and video clips.

4.3. Analysis

To examine the cross-modal interaction, we scrutinize how each clip corresponds to the sentence as a whole and to each word. On the left side in Fig. 7, we find that the degree of interactions is well-calibrated so that it resembles the saliency distribution. Subsequently, we illustrate the fine-grained interaction degree on the right. Although the activations may not be intuitively ranked because of unavailable supervision, we observe that the core words such as "food, Two" are highly activated. Also, as the end token [ED] is regarded as the prototype for the text query in CLIP training [50], we find that [ED] is usually highly activated on moment clips.

4.4. Qualitative Results

In Fig. 6, we plot examples of qualitative results. To compare against previous state-of-the-art methods, we illustrate the plots with [23, 27, 32, 46]. As more accurate moment predictions against other methods are observed in the bar plot, we believe that the plot shows the significance of scaling the degree of clip-wise cross-modal interaction. Furthermore, the line plot showing highlight detection predictions also verifies the effectiveness of exploiting the scaled degree. For additional results, we refer to Appendix A.8.

5. Conclusion

In this paper, we introduced CG-DETR, calibrating the query-dependency of video representation with respect to the correlation between video clips and text query. To enable the calibration of the degree of video-query interaction, we first proposed an adaptive cross-attention equipped with dummy tokens. By granting dummy tokens a role to take the portion of attention between irrelevant video clips and the text query, we modeled the correlation-guided feature interaction. Then, we devised a clip-word correlation learner to discover fine-grained correlation and further calibrate the interaction at the clip-word level. Consequently, given the video clip tokens equipped with calibrated query-dependency, we leverage the moment adaptive saliency token to exploit the discrepancy in the degree of interactions. With extensive experiments and studies, CG-DETR is verified as a strong tool to associate the desired moments with given language descriptions. We hope CG-DETR can provide new insights in terms of modality interaction for the video grounding community.

A. Appendix

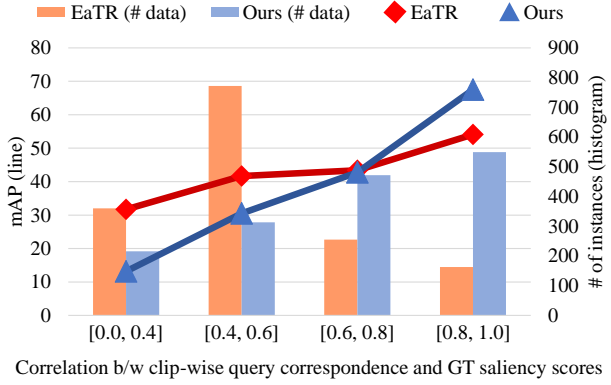


Figure A1. Performance and data count variation across bins of similarity between clip-wise query correspondence (degree of cross-modal interaction) and GT saliency scores. To calculate the similarity between clip-wise-query correspondence and GT saliency scores, we use the cosine similarity. Whereas the histogram displays the number of data points in each interval, the points in the line graph indicate the average score of averaged mAP for moment retrieval in each bin.

A.1. Importance of Considering the Degree of Cross-Modal Interaction

In this section, we illustrate the importance of the degree of cross-modal interaction to support our motivation. Fig. A1 visualizes the positive correlation between how well clip-wise degrees of cross-modal interaction align with the saliency scores and the performance. Along the X-axis, we indicate the range of cosine similarity that is calculated between the ground-truth saliency scores and the degree of cross-modal interaction for each video-text paired data. For each bin in the plot, we calculate the average mAP score for moment retrieval and plot the number of instances that belong to each bin. As shown with the recent work, EaTR, we observe the tendency of performance increase in bins as the degrees of cross-modal interaction resemble the saliency scores which indicates the video-text relevance. By modeling the appropriate correlation during the interaction phase, it is verified with the number of instances in each bin that our model clearly implements the correlation-reflected interaction. Furthermore, as the performance drastically increases along with the quality of injected correlation, we believe that our CG-DETR is a more explainable grounding model compared to previous frameworks.

A.2. When does CG-DETR Benefit the Most: Query Complexity of Datasets

The query complexity of datasets can be defined by the number of semantic words used; we intuitively believe that query

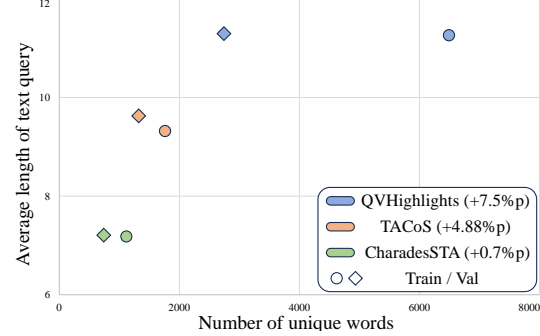


Figure A2. Examined text query complexity of each dataset. X- and Y-axis denote the number of unique words and the average length of text queries in each dataset split, respectively. We state that the query complexity is higher when the number of unique words in each set is bigger and the average query length is longer.

complexity is high if diverse semantic words are used and the average query length is longer. In Fig. A2, we have plotted the text query complexity of each moment retrieval dataset. Comparing the query complexity with the moment retrieval performances (Tab. 1, Tab. 2, and Tab. 3 in the manuscript), we find a strong correlation between the two as indicated in Sec. 4.1 in the manuscript; our moment retrieval results are notable on QVHighlights (7.5%p increase in R1@0.7 compared to [32]) which possess the highest query complexity and relatively less effective on Charades-STA (0.7%p increase in R1@0.7 compared to [32]). This is because our aim is to discover and apply coarse-to-fine correlations between text and video modalities; when dealing with overly simplistic or excessively short text queries containing fewer semantic components, we anticipate a decrease in benefits. Consequently, we claim that CG-DETR benefits the most in cases where language descriptions are semantically rich and the model can infer and exploit diverse correlations between queries and videos.

A.3. Experimental Settings

A.3.1 Datasets

Moment Retrieval. **QVHighlights** is relatively recently publicized dataset by [27]. Consisting of varying lengths of moments and diverse text queries, it is a challenging and only dataset for joint moment retrieval and highlight detection tasks. Providing 10,310 video-text pairs, it provides a test server on Codalab to ensure fair comparisons. **Charades-STA** and **TACoS** are datasets for moment retrieval. Charades-STA [15] consists of 9,848 videos regarding indoor activities with an average duration of 30 seconds. There exist a few benchmarks depending on the type of feature extractors. Among them, we follow [43, 46] to test with two popular backbones, *i.e.*, Slowfast+Clip and VGG. TACoS [51] includes videos mostly about cooking as it is derived from the MPII Cooking Composite Activi-

Dataset	Feat	Hyperparameters						Layer						Loss							
		bs	epoch	lr	lr drop	L_d	L_p	K	Enc.	Dec.	ACA	D.Enc.	Mom.	Sent.	λ_{hl}	λ_{L1}	λ_{gIoU}	λ_{CE}	λ_{ortho}	λ_{align}	$\lambda_{distill}$
QVHighlights	SF+C	32	200	1e-4	x	45	10	1	3	3	2	2	1	1	1	10	1	4	1	1	1
Charades-STA	SF+C	32	200	2e-4	x	45	10	2	3	3	2	2	1	1	4	10	1	4	1	1	1
Charades-STA	VGG	16	200	2e-4	x	45	10	2	3	3	2	2	1	1	4	10	1	4	1	1	1
TACoS	SF+C	32	200	2e-4	x	50	10	2	3	3	2	2	1	1	4	10	1	4	1	1	1
TVSum	I3D	4	1000	1e-3	x	3	10	Tab. A2	3	3	2	2	1	1	4	10	1	4	1	1	1
Youtube-HL	SF+C	4	1000	2e-4	x	1	10	Tab. A3	3	3	2	2	1	1	4	10	1	4	1	1	1

Table A1. Implementation details. From the left to the right, 'bs' denotes the batch size; 'lr' denotes the learning rate; 'lr drop' denotes whether we drop the learning rate or not; L_d denotes the number of dummy tokens; L_p denotes the number of candidates in the moment-representative candidate pool; K denotes the number of selected candidates to form moment-representative saliency token; Enc. denotes the number of transformer encoder layers; Dec. denotes the number of transformer decoder layers; ACA denotes the number of adaptive cross attention layers; D.Enc. denotes the number of dummy encoder layers; Mom. denotes the number of moment encoder layers; Sent. denotes the number of sentence encoder layers.

Domains	VT	VU	GA	MS	PK	PR	FM	BK	BT	DS
K	2	1	1	2	2	2	2	2	1	2

Table A2. Number of selected candidates to form moment-representative saliency token for TVSum.

ties dataset [55]. With 127 cooking videos, it has 18,818 moment-query pairs with an average duration of 287 seconds. Among them, we use 9790 pairs for training and 4436 pairs for testing.

Highlight Detection. **TVSum** and **Youtube-HL** are datasets for highlight detection. TVSUM [61], Title-based Video Summarization dataset, composes 50 videos of various genres, *e.g.*, news, documentary, and vlog. Obtained via crowdsourcing, it has 20 saliency score annotations per video. We follow the settings in [43, 46]. YouTube Highlights [63] is composed of 433 videos from 6 domains: dog, gymnastics, parkour, skating, skiing, and surfing. We follow [32] for the settings, as well as the usage of the domain name as the text query.

A.3.2 Evaluation Metrics

To evaluate moment retrieval, we mainly use Recall@1 (R@1) and Mean Average Precision (mAP) with different IoU thresholds. We also report mean Intersection over Union (mIoU) for Charades-STA, TACoS, and NLQ datasets. For highlight detection, we use mAP for QVHighlights, TVSum, and Youtube-hl following [27, 32, 43, 46]. HIT@1, a metric to compute the hit ratio for the most highlighted clip, is additionally used for QVHighlights.

A.4. Training Details

In this section, we describe the training objectives, hyperparameters, and implementation details.

Training Objectives. As elaborated in the manuscript, CG-DETR consists of two sets of objectives: moment retrieval and highlight detection. To predict the timestamp

Domains	Dog	Gym.	Park.	Ska.	Ski.	Surf.
K	1	1	2	2	1	2

Table A3. Number of selected candidates to form moment-representative saliency token for Youtube-hl.

of the target moments, we utilize L1 and generalized IoU losses [52] with cross-entropy (CE) loss to classify the moment queries between foreground and background. Let us denote the ground-truth moment and binary classification label as $m = (m_c, m_\sigma)$ and y , and corresponding predictions as $\bar{m} = (\bar{m}_c, \bar{m}_\sigma)$ and \bar{y} , respectively, then the objective is formulated as:

$$\mathcal{L}_{\text{mr}} = \lambda_{L1} \mathcal{L}_{L1}(m, \bar{m}) + \lambda_{gIoU} \mathcal{L}_{gIoU}(m, \bar{m}) + \lambda_{CE} L_{CE}(y, \bar{y}), \quad (16)$$

where λ_* stands for the coefficients for corresponding losses.

Margin ranking loss, rank contrastive loss, and entropy loss for negative pairs are used for highlight detection. Among them, margin ranking loss and rank contrastive loss share the objective that ensures the ranking of ground-truth saliency scores is preserved in the predicted scores. Entropy loss for negative pairs is to suppress the saliency scores of unmatched pairs. These losses can be formulated as:

$$\mathcal{L}_{\text{marg}} = \max(0, \Delta + S(v^{\text{low}}) - S(v^{\text{high}})); \quad (17)$$

$$\mathcal{L}_{\text{retl}} = - \sum_{r=1}^R \log \frac{\sum_{v \in V_r^{\text{pos}}} \exp(S(v)/\tau)}{\sum_{v \in (V_r^{\text{pos}} \cup V_r^{\text{neg}})} \exp(S(v)/\tau)}; \quad (18)$$

$$\mathcal{L}_{\text{neg}} = - \log(1 - S(v^{\text{neg}})), \quad (19)$$

$$\mathcal{L}_{\text{hl}} = \mathcal{L}_{\text{marg}} + \mathcal{L}_{\text{retl}} + \mathcal{L}_{\text{neg}}, \quad (20)$$

where Δ , $S(\cdot)$, V^{high} , v^{high} and v^{low} denote a margin, saliency estimation process, and video tokens from pairs of high and low-rank clips, respectively. τ is a temperature scaling parameter and v^{neg} is video token aggregated with unmatched text query.

Consequently, with all the above objectives and the highlight detection losses with attention weights $\mathcal{L}_{\text{attn}}$ combined, our final objective can be formulated as indicated in the

Enc.	Dec.	ACA	D.Enc.	Mom	Sent.	MR			HD			
						R1		mAP		>= Very Good		
						@0.5	@0.7	@0.5	@0.75	Avg.	mAP	HIT@1
2	2	2	2	1	1	65.29	50.32	64.21	43.47	42.79	40.23	65.87
2	2	2	2	2	2	64.13	48.06	64.07	42.81	42.33	39.91	64.84
3	3	2	2	1	1	67.35	52.06	65.57	45.73	44.93	40.79	66.71
3	3	2	2	2	2	66.39	50.90	65.40	46.17	44.92	40.31	66.71
3	3	3	2	2	2	65.87	50.45	65.00	44.61	44.14	40.66	66.13
3	3	3	3	3	3	65.29	50.90	64.85	44.27	43.69	40.62	65.87

Table A4. Layer ablation. In inference time, only the layers for encoder, decoder, adaptive cross-attention, and dummy encoder are used.

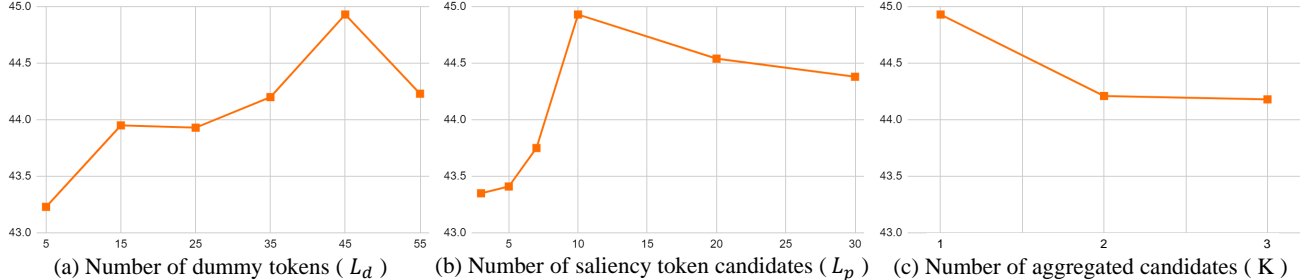


Figure A3. Ablation studies on hyperparameters with averaged mAP metric for moment retrieval task.

manuscript:

$$\mathcal{L}_{obj} = \mathcal{L}_{mr} + \lambda_{hl} (\mathcal{L}_{hl} + \mathcal{L}_{attn} + \mathcal{L}_{bce}) + \lambda_{ortho} \mathcal{L}_{ortho} + \lambda_{align} \mathcal{L}_{align} + \lambda_{distill} \mathcal{L}_{distill}. \quad (21)$$

Hyperparamters. Parameters for each benchmark are enumerated in Tab. A1. Following [27, 43, 46] on QVHighlights, Charades-STA, and TVSum, we utilize slowfast [13], CLIP [50], VGG [58], and I3D [7] backbone features. For TACoS and Youtube-HL datasets, we follow [32] to use slowfast and CLIP. Note that we differ the hyperparameter K per domain for highlight detection datasets as different domains are treated as different splits [32]. Details for these datasets are enumerated in Tab. A2 and Tab. A3. For other details, we use the Adam optimizer with a weight decay of 1e-4 for all experiments. The hidden dimension of the transformer architecture is set to 256, and τ for rank contrastive loss is set to 0.5 for all experiments.

Additional implementation details. Following [32, 46], we also employ a negative-pair learning strategy. However, to alleviate the risk of forming false negative pairs during training, we do not use the video clips from the same video as a negative pair. Moreover, as we regard negative pairs to contain any query-corresponding moments, we do not calculate $\mathcal{L}_{distill}$ with the negative pairs. Lastly, we also adopt modality embedding following [32].

A.5. Ablation Study

Layer. Previous works have demonstrated the effectiveness of the model capacity for temporal grounding [23, 32].

Following them, we also provide the performance variation according to the model size in Tab. A4. As others also observed, we find that the increased capacity in the mainstream, *i.e.*, encoder and decoder, yields higher performances. Yet, we find that the capacity increase in the moment and sentence encoder may result in decreased performance as these encoders learning the alignment between clearly segmented moments and text queries is a much easier task compared to the grounding task that requires clip-level predictions.

Dummy tokens. An ablation study for the number of dummy tokens can be found in Fig. A3 (a). Simply put, as the increased number of dummy tokens can express more complicated patterns, we find that there is a tendency for a performance boost with the increased number of dummies. Yet, we also find that the number of dummies should be determined according to the complexity of patterns in each dataset as too large a number of dummies may disturb the training. For example, in the case of youtube-hl, we empirically find that setting L_d to 1 performs the best since not only examples in each domain are domain-specific but also do not require fine-grained discrimination with complex patterns.

Candidate pool for moment-adaptive saliency token. For the candidate pool, we have two parameters; L_p is the number of token candidates in the pool and K is the number of selected candidates. We conduct an ablation study for these parameters in Fig. A3 (b) and (c). Generally, our model is not very vulnerable to the size of the candidate pool and

Split		test								val							
Method	PT	MR				HD				MR				HD			
		R1		mAP		>= Very Good		R1		mAP		>= Very Good		R1		mAP	
		@0.5	@0.7	@0.5	@0.75	Avg.	mAP	HIT@1	@0.5	@0.7	@0.5	@0.75	Avg.	mAP	HIT@1		
UniVGT [32]	✗	58.86	40.86	57.6	35.59	35.47	38.20	60.96	59.74	-	-	-	36.13	38.83	61.81		
CG-DETR (Ours)	✗	65.43	48.38	64.51	42.77	42.86	40.33	66.21	67.35	52.06	65.57	45.73	44.93	40.79	66.71		
UniVTG [32]	✓	65.43	50.06	64.06	45.02	43.63	40.54	66.28	68.39	-	-	-	45.99	41.25	67.42		
CG-DETR (Ours)	✓	68.48	53.11	69.40	49.12	47.97	40.71	66.60	68.65	54.39	69.47	51.06	49.29	40.55	66.65		

Table A5. Results with large-scale pretraining on QVHighlights *test* and *val* splits. Pretraining was conducted on Ego4D and VideoCC datasets.

Split		test								val							
Method	PT	MR				HD				MR				HD			
		R1		mAP		>= Very Good		R1		mAP		>= Very Good		R1		mAP	
		@0.5	@0.7	@0.5	@0.75	Avg.	mAP	HIT@1	@0.5	@0.7	@0.5	@0.75	Avg.	mAP	HIT@1		
Convolution (Ours)		64.33	46.82	55.55	38.78	37.25	40.92	66.15	66.13	49.1	55.57	39.61	38.01	41.23	66.90		
DETR (Ours)		65.43	48.38	64.51	42.77	42.86	40.33	66.21	67.35	52.06	65.57	45.73	44.93	40.79	66.71		

Table A6. Performance comparison between ours with convolutional decoder and DETR on QVHighlights *test* and *val* splits.

the number of selected candidates. Furthermore, we observe that using the maximum combinations with two tokens out of ten candidates can decently express the diverse characteristics of moment clips in the L_p and K columns in Tab. A1. This validates the idea that matching clips without context helps to efficiently cover varying properties of moment clips with the limited size of the candidate pool.

A.6. Large-scale Pretraining

Recently, as many works have observed the effectiveness of pretraining strategies, a lot of attention is being paid to pre-training strategies. In this subsection, we scrutinize whether our CG-DETR benefits from the pretraining. Particularly, we adopt the recent pretraining technique for temporal grounding [32]. We use Ego4D [17], VideoCC [47] datasets with unified annotations provided by UniVTG¹. Pretraining was conducted on 8 NVIDIA Tesla A100 GPUs.

Results are reported in Tab. A5. As can be seen, our proposed method gains superior performances after pretraining. Compared to the very recent baseline, CG-DETR achieves 10% and 7.2% performance gains with the mAP metric for moment retrieval. Furthermore, ours also shows relatively fewer symptoms of overfitting whereas the performances of the baseline differ in *test* and *val* splits.

A.7. Decoder for Moment Retrieval: Convolution v.s. DETR.

Recent temporal grounding techniques can be categorized into convolution-based and DETR-based. In this subsection, we briefly study the benefits of two types of architecture. In short, each type has its strengths in different circumstances. As can be expected intuitively, the convolution-based model has its advantage when processing the datasets with the

Method	NLQ			
	R@0.3	R@0.5	R@0.7	mIoU
Conv-based (Ours)	7.33	4.16	2.01	5.21
DETR-based (Ours)	6.07	3.10	1.19	4.71

Table A7. Performances of ours with convolutional decoder and DETR on NLQ. Video features are extracted using Slowfast and CLIP.

property of locality whereas the DETR-based is superior in making predictions for more complex datasets. To verify the claim, we implement and compare both versions on QVHighlights and NLQ datasets where their variations in moment lengths vary; QVHighlights is challenging due to the large variation in the length of moments varies from pair to pair and moment length in NLQ does not vary much.

Results are in Tab. A6 and Tab. A7. While the results with DETR architectures are more powerful in more challenging QVHighlights dataset, the convolution decoder shows its strength when locality exists in moment length. To provide detailed statistics for the locality, the standard deviation of moment length is 0.237 for QVHighlights whereas it is 0.046 for NLQ (We normalized every video length to 1 and calculated the standard deviation of portions of the moment). Results for highlight detection with QVHighlights are comparable because they share the encoder architecture where predictions for highlight detection are yielded.

A.8. Visualizations

In Fig. A4, we show additional paired plots of the learned correlation between video clips and text queries at sentence and word levels. Fig. A5, Fig. A6, Fig. A7 visualize additional qualitative comparisons between methods on the QVHighlights dataset.

¹<https://github.com/showlab/UniVTG>

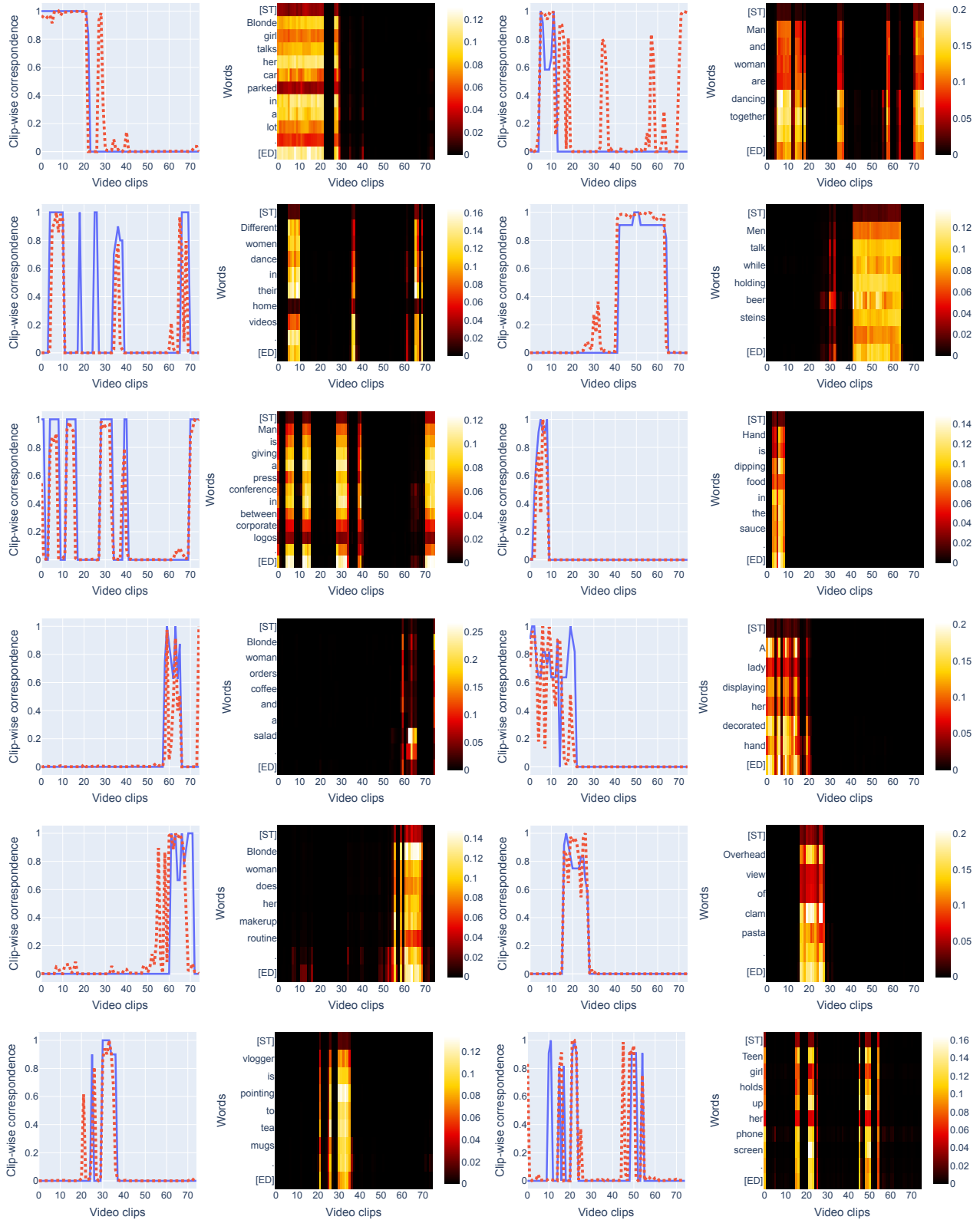
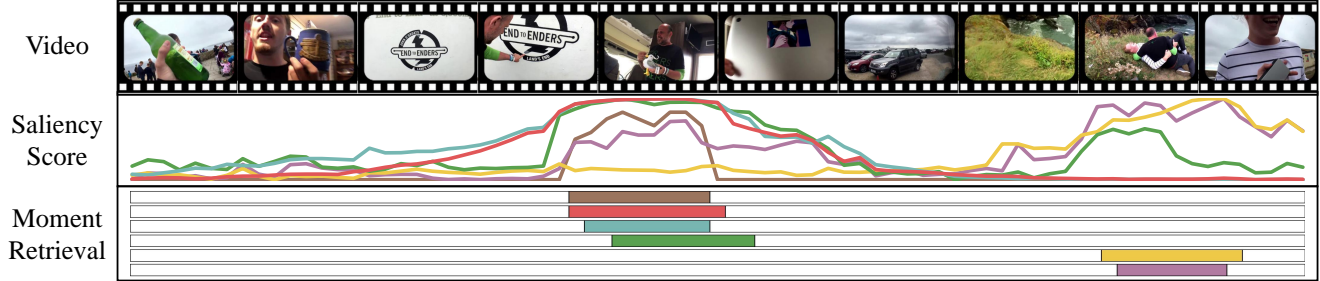


Figure A4. Visualizations of learned correlation between paired video clips and text queries.



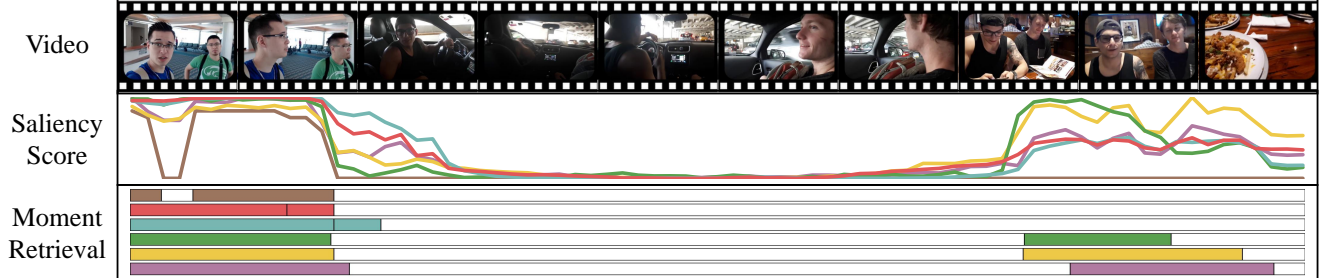
Query: Man is holding a duck on the bus.



Query: A woman holds up her phone near her face with fluffing her hair with her hand.



Query: Two teen boys are in a airport lobby.



Query: Girl is vlogging in a black sweatshirt.



Query: People are skiing and snowboarding down a mountain.

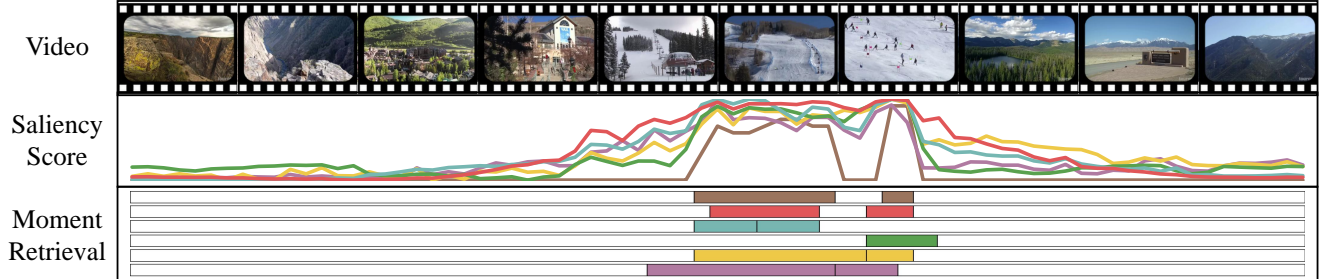
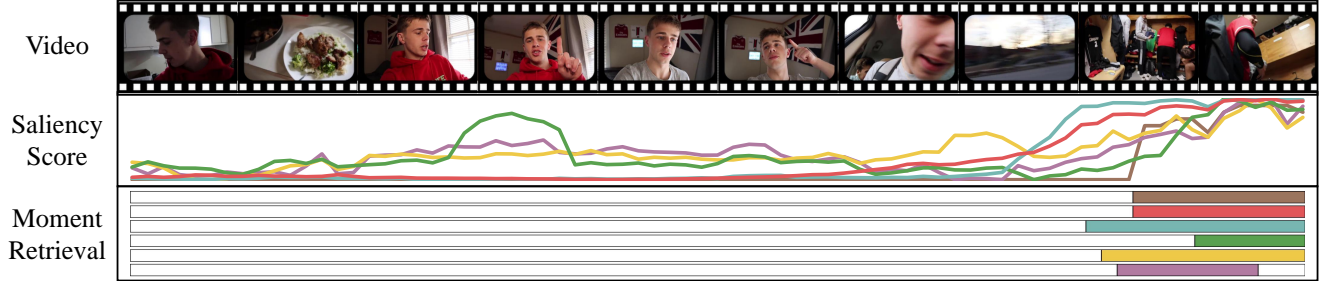


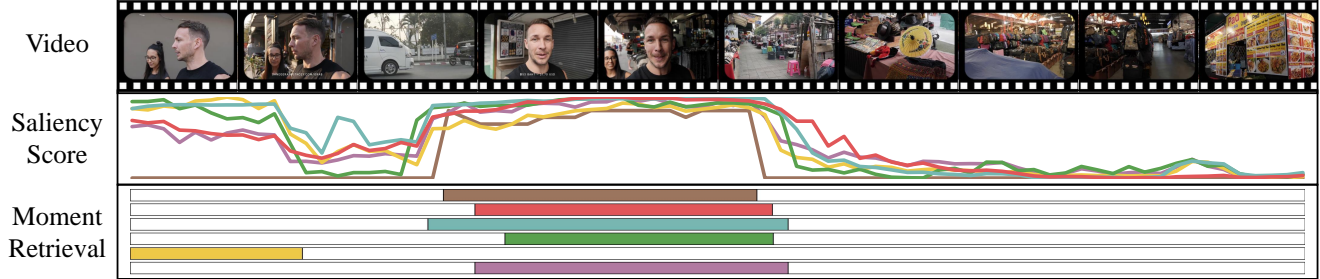
Figure A5. Qualitative results.



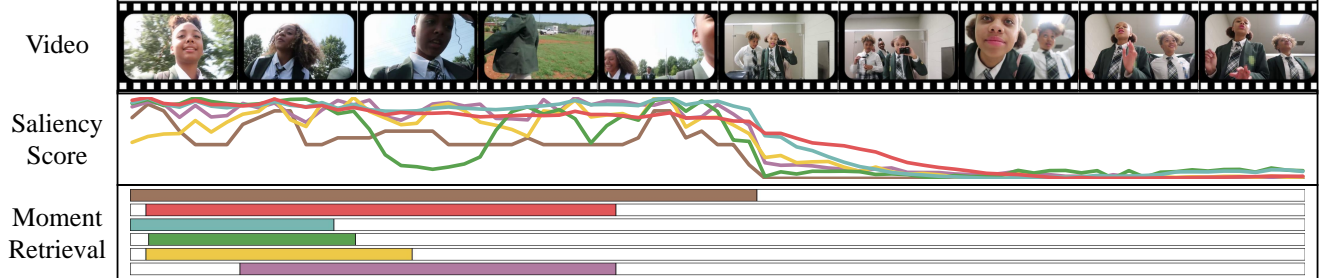
Query: Guys sitting and talking on a locker room



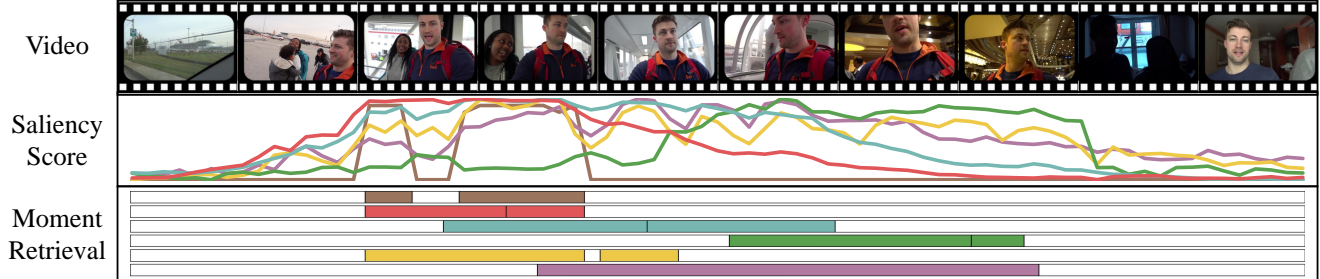
Query: Man wears a black sleeveless shirt while walking with his girlfriend.



Query: A group of children in their school outfits walk through a field together.



Query: Man and woman head through a glass walkway together.



Query: Vlogger fills their car up with gas.

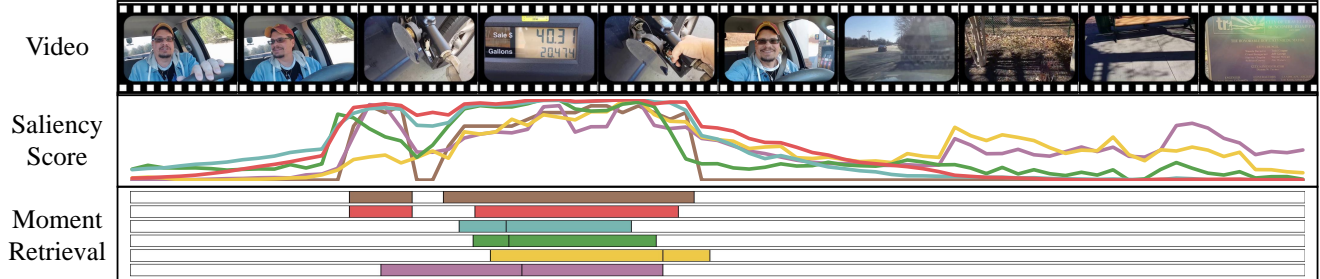


Figure A6. Qualitative results.



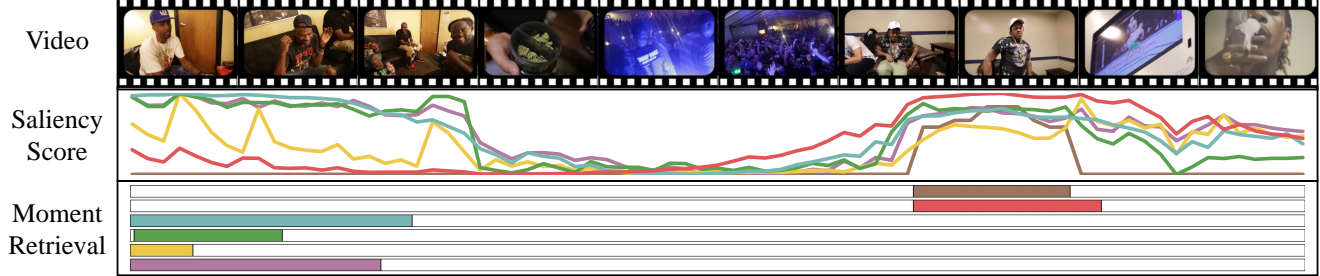
Query: A man in a black shirt and white pants is pacing around a pool.



Query: Woman is wearing a large red scarf.



Query: The man in the white hat talks to the camera and explains who he is.



Query: A press conference is being held at the office of the Rockland County with a grey haired man speaking.



Query: Cartoon of a man in a gray suit talking.



Figure A7. Qualitative results.

References

[1] Lisa Anne Hendricks, Oliver Wang, Eli Shechtman, Josef Sivic, Trevor Darrell, and Bryan Russell. Localizing moments in video with natural language. In *Proceedings of the IEEE international conference on computer vision*, pages 5803–5812, 2017. [2](#), [6](#)

[2] Taivanbat Badamdorj, Mrigank Rochan, Yang Wang, and Li Cheng. Joint visual and audio learning for video highlight detection. In *Proceedings of the IEEE/CVF International Conference on Computer Vision*, pages 8127–8137, 2021. [7](#)

[3] Taivanbat Badamdorj, Mrigank Rochan, Yang Wang, and Li Cheng. Joint visual and audio learning for video highlight detection. In *Proceedings of the IEEE/CVF International Conference on Computer Vision*, pages 8127–8137, 2021. [2](#)

[4] Taivanbat Badamdorj, Mrigank Rochan, Yang Wang, and Li Cheng. Contrastive learning for unsupervised video highlight detection. In *Proceedings of the IEEE/CVF Conference on Computer Vision and Pattern Recognition*, pages 14042–14052, 2022. [2](#)

[5] Wayner Barrios, Mattia Soldan, Fabian Caba Heilbron, Alberto Mario Ceballos-Arroyo, and Bernard Ghanem. Localizing moments in long video via multimodal guidance. In *Proceedings of the IEEE/CVF International Conference on Computer Vision*, 2023. [2](#)

[6] Sijia Cai, Wangmeng Zuo, Larry S Davis, and Lei Zhang. Weakly-supervised video summarization using variational encoder-decoder and web prior. In *Proceedings of the European conference on computer vision (ECCV)*, pages 184–200, 2018. [2](#)

[7] Joao Carreira and Andrew Zisserman. Quo vadis, action recognition? a new model and the kinetics dataset. In *proceedings of the IEEE Conference on Computer Vision and Pattern Recognition*, pages 6299–6308, 2017. [6](#), [11](#)

[8] Jingyuan Chen, Xinpeng Chen, Lin Ma, Zequn Jie, and Tat-Seng Chua. Temporally grounding natural sentence in video. In *Proceedings of the 2018 conference on empirical methods in natural language processing*, pages 162–171, 2018. [2](#)

[9] Shaoxiang Chen and Yu-Gang Jiang. Semantic proposal for activity localization in videos via sentence query. In *Proceedings of the AAAI Conference on Artificial Intelligence*, 2019. [6](#)

[10] Shaoxiang Chen, Wenhao Jiang, Wei Liu, and Yu-Gang Jiang. Learning modality interaction for temporal sentence localization and event captioning in videos. In *Computer Vision–ECCV 2020: 16th European Conference, Glasgow, UK, August 23–28, 2020, Proceedings, Part IV 16*, pages 333–351. Springer, 2020. [2](#)

[11] Ting Chen, Simon Kornblith, Mohammad Norouzi, and Geoffrey Hinton. A simple framework for contrastive learning of visual representations. In *International conference on machine learning*, pages 1597–1607. PMLR, 2020. [4](#)

[12] Victor Escorcia, Mattia Soldan, Josef Sivic, Bernard Ghanem, and Bryan Russell. Temporal localization of moments in video collections with natural language. *arXiv preprint arXiv:1907.12763*, 2019. [6](#)

[13] Christoph Feichtenhofer, Haoqi Fan, Jitendra Malik, and Kaiming He. Slowfast networks for video recognition. In *Proceedings of the IEEE/CVF international conference on computer vision*, pages 6202–6211, 2019. [6](#), [11](#)

[14] Junyu Gao and Changsheng Xu. Fast video moment retrieval. In *Proceedings of the IEEE/CVF International Conference on Computer Vision*, pages 1523–1532, 2021. [6](#)

[15] Jiyang Gao, Chen Sun, Zhenheng Yang, and Ram Nevatia. Tall: Temporal activity localization via language query. In *Proceedings of the IEEE international conference on computer vision*, pages 5267–5275, 2017. [2](#), [6](#), [9](#)

[16] Runzhou Ge, Jiyang Gao, Kan Chen, and Ram Nevatia. Mac: Mining activity concepts for language-based temporal localization. In *2019 IEEE winter conference on applications of computer vision (WACV)*, pages 245–253. IEEE, 2019. [2](#)

[17] Kristen Grauman, Andrew Westbury, Eugene Byrne, Zachary Chavis, Antonino Furnari, Rohit Girdhar, Jackson Hamburger, Hao Jiang, Miao Liu, Xingyu Liu, et al. Ego4d: Around the world in 3,000 hours of egocentric video. In *Proceedings of the IEEE/CVF Conference on Computer Vision and Pattern Recognition*, pages 18995–19012, 2022. [12](#)

[18] Michael Gygli, Yale Song, and Liangliang Cao. Video2gif: Automatic generation of animated gifs from video. In *Proceedings of the IEEE conference on computer vision and pattern recognition*, pages 1001–1009, 2016. [2](#), [7](#)

[19] Michael Gygli, Yale Song, and Liangliang Cao. Video2gif: Automatic generation of animated gifs from video. In *Proceedings of the IEEE conference on computer vision and pattern recognition*, pages 1001–1009, 2016. [2](#)

[20] Lisa Anne Hendricks, Oliver Wang, Eli Shechtman, Josef Sivic, Trevor Darrell, and Bryan Russell. Localizing moments in video with temporal language. In *Proceedings of the 2018 Conference on Empirical Methods in Natural Language Processing*, pages 1380–1390. Association for Computational Linguistics, 2018. [2](#)

[21] Fa-Ting Hong, Xuanteng Huang, Wei-Hong Li, and Wei-Shi Zheng. Mini-net: Multiple instance ranking network for video highlight detection. In *European Conference on Computer Vision*, pages 345–360. Springer, 2020. [2](#)

[22] Fa-Ting Hong, Xuanteng Huang, Wei-Hong Li, and Wei-Shi Zheng. Mini-net: Multiple instance ranking network for video highlight detection. In *European Conference on Computer Vision*, pages 345–360. Springer, 2020. [7](#)

[23] Jinhyun Jang, Jungin Park, Jin Kim, Hyeongjun Kwon, and Kwanghoon Sohn. Knowing where to focus: Event-aware transformer for video grounding. In *Proceedings of the IEEE/CVF International Conference on Computer Vision*, 2023. [2](#), [6](#), [7](#), [8](#), [11](#)

[24] Chao Jia, Yinfei Yang, Ye Xia, Yi-Ting Chen, Zarana Parekh, Hieu Pham, Quoc Le, Yun-Hsuan Sung, Zhen Li, and Tom Duerig. Scaling up visual and vision-language representation learning with noisy text supervision. In *International conference on machine learning*, pages 4904–4916. PMLR, 2021. [2](#)

[25] Aditya Khosla, Raffay Hamid, Chih-Jen Lin, and Neel Sundaresan. Large-scale video summarization using web-image priors. In *Proceedings of the IEEE conference on computer vision and pattern recognition*, pages 2698–2705, 2013. [2](#)

[26] Jie Lei, Licheng Yu, Tamara L Berg, and Mohit Bansal. Tvr: A large-scale dataset for video-subtitle moment retrieval. In

European Conference on Computer Vision, pages 447–463. Springer, 2020. 6

[27] Jie Lei, Tamara L Berg, and Mohit Bansal. Detecting moments and highlights in videos via natural language queries. *Advances in Neural Information Processing Systems*, 34: 11846–11858, 2021. 1, 2, 6, 7, 8, 9, 10, 11

[28] Ang Li, Allan Jabri, Armand Joulin, and Laurens Van Der Maaten. Learning visual n-grams from web data. In *Proceedings of the IEEE International Conference on Computer Vision*, pages 4183–4192, 2017. 2

[29] Junnan Li, Dongxu Li, Caiming Xiong, and Steven Hoi. Blip: Bootstrapping language-image pre-training for unified vision-language understanding and generation. In *International Conference on Machine Learning*, pages 12888–12900. PMLR, 2022.

[30] Junnan Li, Dongxu Li, Silvio Savarese, and Steven Hoi. Blip-2: Bootstrapping language-image pre-training with frozen image encoders and large language models. *arXiv preprint arXiv:2301.12597*, 2023.

[31] Liunian Harold Li, Pengchuan Zhang, Haotian Zhang, Jianwei Yang, Chunyuan Li, Yiwu Zhong, Lijuan Wang, Lu Yuan, Lei Zhang, Jenq-Neng Hwang, et al. Grounded language-image pre-training. In *Proceedings of the IEEE/CVF Conference on Computer Vision and Pattern Recognition*, pages 10965–10975, 2022. 2, 4

[32] Kevin Qinghong Lin, Pengchuan Zhang, Joya Chen, Shraman Pramanick, Difei Gao, Alex Jinpeng Wang, Rui Yan, and Mike Zheng Shou. Univtg: Towards unified video-language temporal grounding. In *Proceedings of the IEEE/CVF International Conference on Computer Vision*, 2023. 1, 2, 6, 7, 8, 9, 10, 11, 12

[33] Zhijie Lin, Zhou Zhao, Zhu Zhang, Zijian Zhang, and Deng Cai. Moment retrieval via cross-modal interaction networks with query reconstruction. *IEEE Transactions on Image Processing*, 29:3750–3762, 2020. 2

[34] Bingbin Liu, Serena Yeung, Edward Chou, De-An Huang, Li Fei-Fei, and Juan Carlos Niebles. Temporal modular networks for retrieving complex compositional activities in videos. In *Proceedings of the European Conference on Computer Vision (ECCV)*, pages 552–568, 2018. 2

[35] Daizong Liu, Xiaoye Qu, Xiao-Yang Liu, Jianfeng Dong, Pan Zhou, and Zichuan Xu. Jointly cross-and self-modal graph attention network for query-based moment localization. In *Proceedings of the 28th ACM International Conference on Multimedia*, pages 4070–4078, 2020. 2

[36] Daizong Liu, Xiaoye Qu, Jianfeng Dong, and Pan Zhou. Adaptive proposal generation network for temporal sentence localization in videos. In *Proceedings of the 2021 Conference on Empirical Methods in Natural Language Processing*, pages 9292–9301, 2021. 6

[37] Daizong Liu, Xiaoye Qu, Jianfeng Dong, Pan Zhou, Yu Cheng, Wei Wei, Zichuan Xu, and Yulai Xie. Context-aware biaffine localizing network for temporal sentence grounding. In *Proceedings of the IEEE/CVF Conference on Computer Vision and Pattern Recognition*, pages 11235–11244, 2021. 2

[38] Meng Liu, Xiang Wang, Liqiang Nie, Xiangnan He, Baoquan Chen, and Tat-Seng Chua. Attentive moment retrieval in videos. In *The 41st international ACM SIGIR conference on research & development in information retrieval*, pages 15–24, 2018. 2

[39] Meng Liu, Liqiang Nie, Yunxiao Wang, Meng Wang, and Yong Rui. A survey on video moment localization. *ACM Computing Surveys*, pages 1–37, 2023. 2

[40] Shilong Liu, Feng Li, Hao Zhang, Xiao Yang, Xianbiao Qi, Hang Su, Jun Zhu, and Lei Zhang. DAB-DETR: Dynamic anchor boxes are better queries for DETR. In *International Conference on Learning Representations*, 2022. 7

[41] Shilong Liu, Zhaoyang Zeng, Tianhe Ren, Feng Li, Hao Zhang, Jie Yang, Chunyuan Li, Jianwei Yang, Hang Su, Jun Zhu, et al. Grounding dino: Marrying dino with grounded pre-training for open-set object detection. *arXiv preprint arXiv:2303.05499*, 2023. 4

[42] Wu Liu, Tao Mei, Yongdong Zhang, Cherry Che, and Jiebo Luo. Multi-task deep visual-semantic embedding for video thumbnail selection. In *Proceedings of the IEEE conference on computer vision and pattern recognition*, pages 3707–3715, 2015. 6

[43] Ye Liu, Siyuan Li, Yang Wu, Chang-Wen Chen, Ying Shan, and Xiaohu Qie. Umt: Unified multi-modal transformers for joint video moment retrieval and highlight detection. In *Proceedings of the IEEE/CVF Conference on Computer Vision and Pattern Recognition*, pages 3042–3051, 2022. 1, 2, 6, 7, 9, 10, 11

[44] Kaijing Ma, Xianghao Zang, Zerun Feng, Han Fang, Chao Ban, Yuhua Wei, Zhongjiang He, Yongxiang Li, and Hao Sun. Llavilo: Boosting video moment retrieval via adapter-based multimodal modeling. In *Proceedings of the IEEE/CVF International Conference on Computer Vision*, pages 2798–2803, 2023. 6

[45] Behrooz Mahasseni, Michael Lam, and Sinisa Todorovic. Unsupervised video summarization with adversarial lstm networks. In *Proceedings of the IEEE conference on Computer Vision and Pattern Recognition*, pages 202–211, 2017. 2, 7

[46] WonJun Moon, Sangeek Hyun, SangUk Park, Dongchan Park, and Jae-Pil Heo. Query-dependent video representation for moment retrieval and highlight detection. In *Proceedings of the IEEE/CVF Conference on Computer Vision and Pattern Recognition*, pages 23023–23033, 2023. 1, 2, 3, 5, 6, 7, 8, 9, 10, 11

[47] Arsha Nagrani, Paul Hongsuck Seo, Bryan Seybold, Anja Hauth, Santiago Manen, Chen Sun, and Cordelia Schmid. Learning audio-video modalities from image captions. In *European Conference on Computer Vision*, pages 407–426. Springer, 2022. 12

[48] Guoshun Nan, Rui Qiao, Yao Xiao, Jun Liu, Sicong Leng, Hao Zhang, and Wei Lu. Interventional video grounding with dual contrastive learning. In *Proceedings of the IEEE/CVF conference on computer vision and pattern recognition*, pages 2765–2775, 2021. 2

[49] Rameswar Panda, Abir Das, Ziyan Wu, Jan Ernst, and Amit K Roy-Chowdhury. Weakly supervised summarization of web videos. In *Proceedings of the IEEE International Conference on Computer Vision*, pages 3657–3666, 2017. 2

[50] Alec Radford, Jong Wook Kim, Chris Hallacy, Aditya Ramesh, Gabriel Goh, Sandhini Agarwal, Girish Sastry,

Amanda Askell, Pamela Mishkin, Jack Clark, et al. Learning transferable visual models from natural language supervision. In *International Conference on Machine Learning*, pages 8748–8763. PMLR, 2021. 2, 4, 6, 8, 11

[51] Michaela Regneri, Marcus Rohrbach, Dominikus Wetzel, Stefan Thater, Bernt Schiele, and Manfred Pinkal. Grounding action descriptions in videos. *Transactions of the Association for Computational Linguistics*, 1:25–36, 2013. 6, 9

[52] Hamid Rezatofighi, Nathan Tsoi, JunYoung Gwak, Amir Sadeghian, Ian Reid, and Silvio Savarese. Generalized intersection over union: A metric and a loss for bounding box regression. In *Proceedings of the IEEE/CVF conference on computer vision and pattern recognition*, pages 658–666, 2019. 6, 10

[53] Mrigank Rochan, Linwei Ye, and Yang Wang. Video summarization using fully convolutional sequence networks. In *Proceedings of the European conference on computer vision (ECCV)*, pages 347–363, 2018. 2

[54] Mrigank Rochan, Mahesh Kumar Krishna Reddy, Linwei Ye, and Yang Wang. Adaptive video highlight detection by learning from user history. In *European conference on computer vision*, pages 261–278. Springer, 2020. 2

[55] Marcus Rohrbach, Michaela Regneri, Mykhaylo Andriluka, Sikandar Amin, Manfred Pinkal, and Bernt Schiele. Script data for attribute-based recognition of composite activities. In *Computer Vision–ECCV 2012: 12th European Conference on Computer Vision, Florence, Italy, October 7–13, 2012, Proceedings, Part I 12*, pages 144–157. Springer, 2012. 10

[56] Dian Shao, Yu Xiong, Yue Zhao, Qingqiu Huang, Yu Qiao, and Dahua Lin. Find and focus: Retrieve and localize video events with natural language queries. In *Proceedings of the European Conference on Computer Vision (ECCV)*, pages 200–216, 2018. 2

[57] Karen Simonyan and Andrew Zisserman. Very deep convolutional networks for large-scale image recognition. *arXiv preprint arXiv:1409.1556*, 2014. 6

[58] Karen Simonyan and Andrew Zisserman. Very deep convolutional networks for large-scale image recognition. In *3rd International Conference on Learning Representations (ICLR 2015)*, 2015. 11

[59] Mattia Soldan, Mengmeng Xu, Sisi Qu, Jesper Tegner, and Bernard Ghanem. Vlg-net: Video-language graph matching network for video grounding. In *Proceedings of the IEEE/CVF International Conference on Computer Vision*, pages 3224–3234, 2021. 2

[60] Juyong Song and Sunghyun Choi. Image-text alignment using adaptive cross-attention with transformer encoder for scene graphs. 2021. 3

[61] Yale Song, Jordi Vallmitjana, Amanda Stent, and Alejandro Jaimes. Tvsun: Summarizing web videos using titles. In *Proceedings of the IEEE conference on computer vision and pattern recognition*, pages 5179–5187, 2015. 6, 10

[62] Yale Song, Miriam Redi, Jordi Vallmitjana, and Alejandro Jaimes. To click or not to click: Automatic selection of beautiful thumbnails from videos. In *Proceedings of the 25th ACM international on conference on information and knowledge management*, pages 659–668, 2016. 6

[63] Min Sun, Ali Farhadi, and Steve Seitz. Ranking domain-specific highlights by analyzing edited videos. In *Computer Vision–ECCV 2014: 13th European Conference, Zurich, Switzerland, September 6–12, 2014, Proceedings, Part I 13*, pages 787–802. Springer, 2014. 2, 6, 7, 10

[64] Ashish Vaswani, Noam Shazeer, Niki Parmar, Jakob Uszkoreit, Llion Jones, Aidan N Gomez, Łukasz Kaiser, and Illia Polosukhin. Attention is all you need. *Advances in neural information processing systems*, 30, 2017. 1

[65] Lezi Wang, Dong Liu, Rohit Puri, and Dimitris N Metaxas. Learning trailer moments in full-length movies with co-contrastive attention. In *European Conference on Computer Vision*, pages 300–316. Springer, 2020. 7

[66] Weining Wang, Yan Huang, and Liang Wang. Language-driven temporal activity localization: A semantic matching reinforcement learning model. In *Proceedings of the IEEE/CVF conference on computer vision and pattern recognition*, pages 334–343, 2019. 6

[67] Shaoning Xiao, Long Chen, Songyang Zhang, Wei Ji, Jian Shao, Lu Ye, and Jun Xiao. Boundary proposal network for two-stage natural language video localization. In *Proceedings of the AAAI Conference on Artificial Intelligence*, pages 2986–2994, 2021. 2

[68] Bo Xiong, Yannis Kalantidis, Deepti Ghadiyaram, and Kristen Grauman. Less is more: Learning highlight detection from video duration. In *Proceedings of the IEEE/CVF conference on computer vision and pattern recognition*, pages 1258–1267, 2019. 2, 7

[69] Huijuan Xu, Kun He, Bryan A Plummer, Leonid Sigal, Stan Sclaroff, and Kate Saenko. Multilevel language and vision integration for text-to-clip retrieval. In *Proceedings of the AAAI Conference on Artificial Intelligence*, pages 9062–9069, 2019. 2

[70] Minghao Xu, Hang Wang, Bingbing Ni, Riheng Zhu, Zhenbang Sun, and Changhu Wang. Cross-category video highlight detection via set-based learning. In *Proceedings of the IEEE/CVF International Conference on Computer Vision*, pages 7970–7979, 2021. 2, 7

[71] Yifang Xu, Yunzhuo Sun, Yang Li, Yilei Shi, Xiaoxiang Zhu, and Sidan Du. Mh-detr: Video moment and highlight detection with cross-modal transformer. *arXiv preprint arXiv:2305.00355*, 2023. 1

[72] Shen Yan, Xuehan Xiong, Arsha Nagrani, Anurag Arnab, Zhonghao Wang, Weina Ge, David Ross, and Cordelia Schmid. Unloc: A unified framework for video localization tasks. In *Proceedings of the IEEE/CVF International Conference on Computer Vision*, 2023. 2

[73] Huan Yang, Baoyuan Wang, Stephen Lin, David Wipf, Minyi Guo, and Baining Guo. Unsupervised extraction of video highlights via robust recurrent auto-encoders. In *Proceedings of the IEEE international conference on computer vision*, pages 4633–4641, 2015. 7

[74] Qinghao Ye, Xiyue Shen, Yuan Gao, Zirui Wang, Qi Bi, Ping Li, and Guang Yang. Temporal cue guided video highlight detection with low-rank audio-visual fusion. In *Proceedings of the IEEE/CVF International Conference on Computer Vision*, pages 7950–7959, 2021. 7

[75] Jiahui Yu, Zirui Wang, Vijay Vasudevan, Legg Yeung, Morteza Seyedhosseini, and Yonghui Wu. Coca: Contrastive captioners are image-text foundation models. *Transactions on Machine Learning Research*, 2022. 2

[76] Shoubin Yu, Jaemin Cho, Prateek Yadav, and Mohit Bansal. Self-chained image-language model for video localization and question answering. *Advances in Neural Information Processing Systems*, 2023. 2

[77] Yitian Yuan, Lin Ma, Jingwen Wang, Wei Liu, and Wenwu Zhu. Semantic conditioned dynamic modulation for temporal sentence grounding in videos. *Advances in Neural Information Processing Systems*, 32, 2019. 2

[78] Runhao Zeng, Haoming Xu, Wenbing Huang, Peihao Chen, Mingkui Tan, and Chuang Gan. Dense regression network for video grounding. In *Proceedings of the IEEE/CVF Conference on Computer Vision and Pattern Recognition*, pages 10287–10296, 2020. 2

[79] Da Zhang, Xiyang Dai, Xin Wang, Yuan-Fang Wang, and Larry S Davis. Man: Moment alignment network for natural language moment retrieval via iterative graph adjustment. In *Proceedings of the IEEE/CVF Conference on Computer Vision and Pattern Recognition*, pages 1247–1257, 2019. 2

[80] Hao Zhang, Aixin Sun, Wei Jing, and Joey Tianyi Zhou. Span-based localizing network for natural language video localization. In *Proceedings of the 58th Annual Meeting of the Association for Computational Linguistics*, pages 6543–6554, Online, 2020. Association for Computational Linguistics. 6

[81] Ke Zhang, Wei-Lun Chao, Fei Sha, and Kristen Grauman. Video summarization with long short-term memory. In *European conference on computer vision*, pages 766–782. Springer, 2016. 7

[82] Songyang Zhang, Jinsong Su, and Jiebo Luo. Exploiting temporal relationships in video moment localization with natural language. In *Proceedings of the 27th ACM International Conference on Multimedia*, pages 1230–1238, 2019. 2

[83] Songyang Zhang, Houwen Peng, Jianlong Fu, and Jiebo Luo. Learning 2d temporal adjacent networks for moment localization with natural language. In *Proceedings of the AAAI Conference on Artificial Intelligence*, pages 12870–12877, 2020. 6

[84] Songyang Zhang, Houwen Peng, Jianlong Fu, and Jiebo Luo. Learning 2d temporal adjacent networks for moment localization with natural language. In *Proceedings of the AAAI Conference on Artificial Intelligence*, pages 12870–12877, 2020. 2

[85] Zhu Zhang, Zhijie Lin, Zhou Zhao, and Zhenxin Xiao. Cross-modal interaction networks for query-based moment retrieval in videos. In *Proceedings of the 42nd International ACM SIGIR Conference on Research and Development in Information Retrieval*, pages 655–664, 2019. 2

[86] Hou Zhijian, Ngo Chong-Wah, and Wing-Kwong Chan. Conquer: Contextual query-aware ranking for video corpus moment retrieval. In *Proceedings of the 29th ACM International Conference on Multimedia*, 2021. 2

[87] Jiahao Zhu, Daizong Liu, Pan Zhou, Xing Di, Yu Cheng, Song Yang, Wenzheng Xu, Zichuan Xu, Yao Wan, Lichao Sun, et al. Rethinking the video sampling and reasoning strategies for temporal sentence grounding. In *Findings of the Association for Computational Linguistics: EMNLP 2022*, pages 590–600, 2022. 6

[88] Jiahao Zhu, Daizong Liu, Pan Zhou, Xing Di, Yu Cheng, Song Yang, Wenzheng Xu, Zichuan Xu, Yao Wan, Lichao Sun, et al. Rethinking the video sampling and reasoning strategies for temporal sentence grounding. In *Findings of the Association for Computational Linguistics: EMNLP 2022*, 2022. 2